5.
Circulation modelling

CHAPTER COORDINATOR

Stefania Ciliberti

CHAPTER AUTHORS *(in alphabetical order)*

Nadia Ayoub, Jérôme Chanut, Mauro Cirano, Anne Delamarche, Pierre De Mey-Frémaux, Marie Drévillon, Yann Drillet, Helene Hewitt, Simona Masina, Clemente Tanajura, Vassilios Vervatis, and Liying Wan

5. Circulation modelling

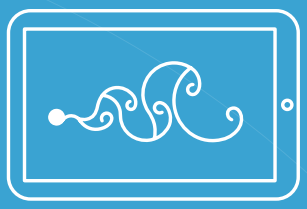

5.1. General introduction to circulation models

5.1.1. Objective, applications and beneficiaries

5.1.2. Circulation Physics

5.2. Circulation forecast and multi-year systems

5.2.1. Ocean-Earth system as basis for OOFS

5.2.2. Architecture singularities

5.3. Input data

5.4. Modelling component: general circulation models

5.4.1. Mathematical model

5.4.2. Basic discretization techniques

5.4.2.1. Horizontal grids

5.4.2.2. Vertical discretization

5.4.2.3. Time stepping

5.4.2.4. Numerical techniques

5.4.3. List of Ocean General Circulation Models

5.4.4. Downscaling large-scale solutions to regional/coastal circulation models

5.5. Data assimilation systems

5.5.1. Basic concepts

5.5.2. Sequential methods

5.5.3. Variational methods

5.5.4. Modelling errors

5.5.5. Overview of current data assimilation systems in operational forecasting

5.6. Ensemble modelling

5.6.1. Basic concepts

5.6.2. Ocean model uncertainties

5.6.3. Towards ocean EPS

5.1. General introduction to circulation models

5.1.1. Objective, applications and beneficiaries

The main objective of any OOFS is to provide users with the best reliable and easy access information available on the state of the ocean in near real-time. The service is meant for any user, and especially downstream service providers who use the information as an input to their own value-added services.

A forecasting system relies on a numerical ocean model and, in many cases, on a data assimilation component able to assimilate the available observations and provide a complete dataset that can be used as initial conditions by the ocean circulation model. The availability of relevant observations is crucial to the success of an OOFS and the development of models and numerical techniques, along with data assimilation schemes that combine all the information taking into account the uncertainties of the observations and models.

The circulation modelling component represents one of the main cores of operational marine monitoring and forecasting systems: it provides an overall description of ocean physical essential variables (i.e. temperature, salinity, currents, sea surface height, etc.) for ocean predictions and for supporting climate studies. Ocean models are able to describe the sea state from global to coastal scales and to predict its variability and evolution in time (from short to mid-term to long-term). This is done by numerically solving a set of partial differential equations, based on an approximated version of the Navier-Stokes equations.

At the beginning of the XX century, Bjerknes (1914) described a practical method that could solve the mathematical dynamic and thermodynamic equations at least for a finite amount of time. He defined two factors that were necessary to make predictions a reality: (1) knowledge of the initial conditions as accurately as possible, and (2) the development of an accurate predictive model. The latter consisted of discretizing the equations and using numerical methods to solve for the time derivative. Based on this approach, the first successful meteorological forecast became operational at the end of the 1960s, while ocean forecasting began in the 1980s; a joint venture between Harvard University and the Naval Postgraduate School in Monterey, both in the United States, completed the first successful forecast of ocean mesoscales in a limited ocean area (see Pinardi et al., 2017, for an overview of the ocean prediction science). Earlier examples of wave forecasting during the second World War responded to the need to know the sea state during landing operations (O'Brien and Johnson, 1947).

During the last decades of the 20th century and the first decades of the 21st century, ocean forecasting has become an operational activity and, thanks to the increase of computing power, today we are able to numerically integrate the governing equations at very high resolution in space and time, to study multi-scale ocean processes, physical properties and their impacts on the climate, and human activities affecting the environment. In modern ocean prediction, stochastic approaches and ensemble estimates complement deterministic solutions, accounting for the different sources of uncertainties (e.g. errors in the initial conditions, in the forcing functions, in the physics of the numerical model, and in the bathymetry) that unavoidably affects the final solution and tends to increase over the forecast period.

To improve the quality of predictions, data assimilation and ensemble techniques are widely used, and their primary scope is to rigorously and systematically combine available observations (in situ and satellite) with numerical ocean models to provide the best estimate of the forecasting cycle. However, in case of very high-resolution nested models and when observation availability is limited, operational systems do not use a data assimilation procedure. When possible, an OOFS system needs to retrieve data observations from a wide variety of observing platforms and systems over the domain of interest for prediction. Satellite based observing systems provide a large source of observational data for an OOFS as well.

An OOFS needs to access information from a numerical weather prediction system in order to provide surface boundary forcing information. The OOFS will also require information on other parameters that influence the ocean such as river outflows, etc. Depending on the domain of interest, the OOFS may also require information about sea ice (see Section 4.2 for the input data and Chapter 6 for understanding sea ice modelling basics). Observations are also used to provide a quantitative understanding of the capacity of the ocean model to make predictions by means of validation and calibration techniques and, consequently, to measure and monitor the accuracy of the forecasting product (see Section 4.5). Routine validation and verification information will tell the OOFS operators when a model is not performing well. The errors identified through validation and verification can be used to set priorities for further development of the OOFS. Despite the enormous improvements reached nowadays by operational forecasting systems ranging from global to coastal scales, much research is still needed to advance in ocean prediction. Developments include access to additional innovative autonomous multi-scale observing technologies observations, both remote and in situ (Le Traon et al., 2019), to new model developments (Fox-Kemper et al., 2019), up to next-generation computational methods and data assimilation schemes supported by the recently expanding applica-

tions of machine learning techniques in this field (De Mey-Frémaux et al., 2019).

The ultimate purpose for operating an OOFS is the production, preparation, and delivery of operational ocean forecasts to users in forms that meet their needs. There is a growing list of users relying on the products and services from operational ocean forecasting systems. Ocean predictions will continue to produce an increasing number of marine applications and services: e.g. for maritime safety, marine resources, coastal and marine environment (Chapter 11). This is because the new systems allow informed management and emergency decisions to be made based on physical knowledge resolved at unprecedented space and time resolution, with known quality and accuracy.

The emergence of operational organisations for delivering real-time forecasts and analyses will encourage the development of value-added products, including forecasts for extreme weather driven events (such as storm surges), pollution, oil spills, acoustic properties (e.g. the speed of sound), sea ice, ecosystem management, safe offshore activities, search and rescue operations, optimal energy extraction, and maritime safety and transport. In addition, ocean forecast products and services can also be providers of information for aquaculture, fishery research, and regional fishery organisations, contributing to the protection and sustainable management of living marine resources. Availability of predictions on the ocean helps to limit damages in the case of floods, storm surges, heat waves and other dangers associated with sea conditions. Furthermore, detailed and accurate forecasts are also useful to assist decision making to plan long-term strategies aiming at managing the risks associated with the impacts of climate change on the sea and coasts, such as sea level rise and marine heat waves.

A predicted ocean where society has the capacity to understand current and future ocean conditions is one of the proposed seven outcomes of the United Nations Decade of Ocean Sciences for Sustainable Development.

Scope of this chapter is to present all elements that make an OOFS and provides a detailed understanding of the main circulation modelling components. For each component, a comprehensive description is provided in dedicated chapter subsections, including the presentation of some state-of-the-art examples of ocean models currently working in operational frameworks. In addition, basic concepts of data assimilation systems and validation strategies will be presented as well, since an essential part of operating a model is to conduct the necessary validation and verification procedures to maintain a continuous quality control of the system outputs.

5.1.2. Circulation Physics

The physical processes, properties and circulation of the ocean are described numerically by the approximated Navier-Stokes equations (details in Section 5.4.1). The equations allow the spatial and temporal distribution of the temperature, salinity, density, pressure, and currents to be described. Numerical ocean models are the building block of operational oceanography and fundamental for near real time to seasonal to decadal forecasts and climate projections. In operational oceanography, they are used alongside data assimilation techniques to accurately represent the state of the ocean at a particular point in time and space, and to produce the initial condition of the forecasting system.

The governing equations for a real fluid are the Navier-Stokes equations, together with conservation of salt and heat and an equation of state; these equations support fast acoustic modes and involve nonlinearities in many terms that make their solution both difficult and expensive. A series of approximations are made to simplify and yield the “primitive equations”, which are the basis of most general circulation models. The assumptions that are made in ocean models are described in Section 5.4.

Ocean circulation models aim to represent key processes. These include: 1) transport of heat by the ocean; 2) the effect of evaporation, precipitation and runoff on ocean salinity and density; and 3) the role of ocean currents which, along with wind waves and tides, drive ocean mixing and water mass transformation. Ocean circulation models discretize the governing equations on a horizontal and vertical grid (Section 5.4 expands on this). The details of whether processes can be explicitly resolved in models or they must be parameterised depend on the resolution of the grid used to solve the approximate numerical system.

Figure 3.4 (see Chapter 3) shows the order of magnitude of spatial and temporal scales of specific ocean processes. If the model resolves scales of 100 km, ocean models should be able to resolve Kelvin and Rossby waves; indeed, the representation of Equatorial dynamics has been shown to be important for forecasting the evolution of El Nino on seasonal timescales (Latif et al., 1994). On shorter timescales but with similar spatial scales, surface tides are key processes to represent. Moving to spatial scales of ~10 km to 100 km, the ocean mesoscale can start to be represented; this scale includes boundary currents and mesoscale eddies (Hewitt et al., 2020). At even finer scales, coastal upwelling, internal tides, and internal waves can be represented. Interactions with bathymetry can be important at the scale of the bathymetry. For example, choke points can determine the exchange between the deep ocean and inland seas, such as the Gibraltar Strait. Horizontal resolution choices are discussed further in Section 5.4.

While a primary consideration is the horizontal scales (Figure 3.4), the choice of vertical resolution and coordinate is also an important consideration. These choices are discussed further in Section 5.4, along with the numerical methods that are employed to solve the equations and some of the parameterisation choices to be made.

The ocean has strong links to other aspects of the Earth system, such as sea ice, which is particularly important for modulating temperature and salinity at high latitudes. Global ocean models include a sea ice component. State-of-the-art sea ice models represent the ice thermodynamics including melt-ponds and the ice dynamics, with a representation of the ice rheology. Many sea ice models also capture the variations in ice thickness or ice age within a typical ocean grid box. Current status of sea ice modelling and the applicability of models for operational forecasting is discussed in Hunke et al. (2020).

This chapter provides complementary information on the way to set an OOFS, which core is the circulation model. Section 5.3 will provide a list of input data needed for setting up an ocean model, from static datasets such the bathymetry to operational products such atmospheric forcing, to other OOFS for the provisioning of initial/boundary conditions in case of regional/coastal models, to observations used for assimilation and validation. Section 5.4 focuses on the mathematical formulation of the primitive equations, providing some basic information to numerical methods for discretization and numerical integration of such equations. Section 5.5 is devoted to presenting the basic mathematics for the data assimilation schemes commonly used in global and regional OOFS. Section 5.6 deals with ensemble modelling and, finally, Sections 5.7 and 5.8 provide major details on the validation approaches and the OOFS output. The last part of this chapter provides an inventory of OOFS, including multi-year systems, operating at international level, from global to coastal scale.

5.2. Circulation forecast and multi-year systems

5.2.1. Ocean-Earth system as basis for OOFS

The ocean is a system that interacts with other systems. Figure 5.1 shows a simplified representation of the Earth system interaction in weather and ocean forecasting. Focusing on the ocean, we can identify (Madec et al., 2022):

- **Connection with land:** in particular with rivers and lakes which exchange freshwater flux with the ocean;
- **Connection with the atmosphere:** the ocean receives precipitation and returns evaporation. The atmosphere and the ocean also exchange horizontal momentum (wind stress) and heat;
- **Connection with sea ice:** the ocean exchanges heat, salt, freshwater and momentum with sea ice. The sea surface temperature is constrained to be at the freezing point of the interface. Sea ice salinity is very low (~4-6 PSU) compared to that of the ocean (~34 PSU). The cycle of freezing/melting is associated with freshwater and salt fluxes and cannot be neglected;
- **Connection with solid earth:** heat and salt fluxes through the seafloor are small, hence no flux of heat and salt is considered across solid boundaries. For momentum instead, we express the kinematic boundary condition. Additionally, the ocean exchanges momentum with the Earth through friction; this needs to be parameterized in terms of turbulent fluxes using bottom and lateral boundary conditions.

These connections will be detailed along this chapter and represent the core of the OOFS architecture introduced in the next subsection.

5.2.2. Architecture singularities

An OOFS that would provide the prediction, as well as the past reconstruction of the past state of the ocean, is based on several components that are strongly linked. A general introduction to OOFS architecture singularities is provided in Chapter 4, which includes for each system component, input and output data, as well as links between some of the components, are described. Complexity of the system, components of the system, infrastructure, maintenance of the code, and monitoring of the whole data flow should be defined depending on needs, robustness and operationality. Of course, the cost of the development, maintenance and evolution of the system depends on operational constraints.

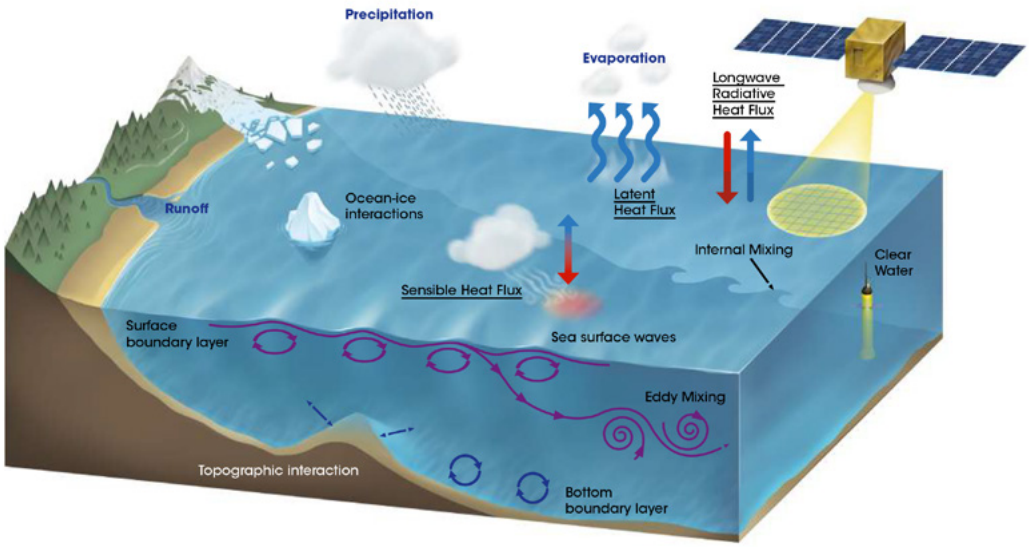

Figure 5.1. Representation of the ocean processes and connections with the Earth.

5.3. Input data

Elements needed to run a circulation model for operational forecasting:

- **Observations.** These are used for:
  - Validation (including forecast verification) and calibration, further described in Section 5.7;
  - Data assimilation, which basic concepts are introduced in Section 5.5;

  Sources of observations are:

  - In-situ observations for the following variables: temperature, salinity, sea surface height, and sea surface currents. See Section 4.2.2. for more information on in-situ ocean observations;
  - Satellite observations for the following list of variables: sea level anomaly, sea surface temperature, and sea ice concentration. Recently, other parameters such as sea surface salinity and sea ice thickness have been remotely measured. See Section 4.2.2. for more information on in-situ ocean observations.

- **Bathymetry.** It is an indispensable topographical information for an Ocean Circulation Forecasting System. Its resolution may significantly drive the modeller during the setup of the circulation model to address specific scales and resolution. For example, in coastal models we may need bathymetric datasets, whose resolution can be even lower than 100 m, to properly represent the physical structural peculiarities of both coastline and shelf area, allowing the representation of small-scale physics. See more information on bathymetric data sets in Section 4.2.4.

- **Atmospheric forcing.** Generated by NWP services, it is vital to provide momentum, heat, and freshwater fluxes to the OOFS. More info on atmospheric forcing can be found in Section 4.2.5.

- **Land forcing.** Provides freshwater fluxes from rivers. More details on this data source are in Section 4.2.6.

- **Initial and boundary conditions from other OOFS.** 3D fields from parent models are required when downscaling to obtain higher resolutions (see Sections 4.2.7. and 5.4.4. for more information).

- **Climatological fields.** These serve as complement to the other data sources or might be used to substitute the previous if no other data are available. See Section 4.2.8 for more information on climatologies.

5.4. Modelling component: general circulation models

An ocean model is a numerical and computational tool used to understand and predict ocean variables (Griffies, 2006), providing a discrete solution of the geophysical fluid dynamic equations. It represents a rigorous way of linking the ocean state parameters through mathematical equations representing the physics that governs the oceans.

In the next subsections, we will introduce the different components of an OGCM, that is part of the OOFS (steps 1 and 2 as in Figure 4.1), focusing on mathematical equations, numerical methods, and spatial discretization techniques. A list of available numerical ocean models is provided in Table 5.1 in Section 5.4.3. Data assimilation methods used in OOFSs are instead presented in Section 5.5.

5.4.1. Mathematical model

The Navier-Stokes equations represent the fundamental laws of fluid dynamics; they are based on conservation of momentum, conservation of mass, and an equation of state.

Oceans are also represented by the following equations (although with some significant simplifications as explained in Madec et al., 2022):

- **Spherical Earth approximation:** the geopotential surfaces are assumed to be oblate spheroids that follow the Earth's bulge, and are approximated by spheres which gravity is locally vertical (parallel to the Earth's radius) and independent from latitude;

- **Thin-shell approximation:** the ocean depth is neglected compared to the Earth's radius;

- **Turbulent closure hypothesis:** the turbulent fluxes - which represent the effect of small-scale processes on the large scale - are expressed in terms of large scale features;

- **Boussinesq hypothesis:** density variations are neglected, except in their contribution to buoyancy force:

$$\rho = \rho(T, S, p) \tag{5.1}$$

- **Hydrostatic hypothesis:** the vertical momentum equation is reduced to a balance between the vertical pressure gradient and the buoyancy force (this removes convective processes from the initial Navier-Stokes equations and so convective processes must be parameterized instead):

$$\frac{\partial p}{\partial z} = -\rho g \tag{5.2}$$

- **Incompressibility hypothesis:** the 3D divergence of the velocity vector U is assumed to be zero:

$$\nabla \cdot U = 0 \tag{5.3}$$

- **Neglect of additional Coriolis terms:** the Coriolis terms that vary with the cosine of latitude are neglected.

Because the gravitational force dominates in the equations of large-scale motions, it is useful to choose an orthogonal set of unit vectors (i,j,k) linked to the Earth such that k is the local upward vector and (i,j) are 2 vectors orthogonal to k. Let us define additionally: U the vector velocity, T the potential temperature, S the salinity, ρ the insitu density. The vector invariant form of the primitive equations in the (i,j,k) vector system provides the following equations:

- The momentum balance:

$$\frac{\partial U_h}{\partial t} = -\left[(\nabla \times U) \times U + \frac{1}{2}\nabla(U^2)\right]_h - fk \times U_h - \frac{1}{\rho_0}\nabla_h p + D^U + F^U \tag{5.4}$$

- The heat and salt conservation equations:

$$\frac{\partial T}{\partial t} = -\nabla \cdot (TU) + D^T + F^T \tag{5.5}$$

$$\frac{\partial S}{\partial t} = -\nabla \cdot (SU) + D^S + F^S \tag{5.6}$$

where ∇ is the generalised derivative vector operator in (i,j,k) directions, t is the time, z is the vertical coordinate, ρ is the in-situ density given by Eq. 5.1, ρ_0 is the reference density, p is the pressure, f$=2\Omega \cdot k$ is the Coriolis acceleration (where Ω is the Earth's angular velocity vector) and g is the gravitational acceleration. D^U, D^T and D^S are the parameterizations of small-scale physics for momentum, temperature and salinity, while F^U, F^T and F^S are surface forcing terms.

OGCMs are able to resolve the mesoscale in some regions but not in others; additionally, once applied for climate research, they cannot entirely reproduce the rich mesoscale eddy activity we observe in reality. For this reason, mixing associated with sub-grid scale turbulence needs to be parameterized.

A common problem an ocean modeller is facing when he/she deals with primitive equations is the numerical discretization in space and time. As described in Hallberg (2013), numerical ocean models need to represent the effects of mesoscale eddies, which are the typical horizontal scales of less than 100 km and timescales in the order of a month. When defining the spatial grid for the numerical integration of the primitive equations, it is important to account for the ratio of a model's grid spacing to the deformation radius, defined as:

$$L_{Def} = \sqrt{\frac{c_g^2}{f^2 + 2\beta c_g}} \tag{5.7}$$

where c_g is the first-mode internal gravity wave speed, f is again the Coriolis parameter, and β is its meridional gradient (Chelton et al., 1998).

Figure 5.2 shows the ocean model resolution required for the baroclinic deformation radius to be twice the grid spacing, based on an eddy-permitting ocean model after one year of spin-up from climatology (Hallberg, 2013).

5.4.2. Basic discretization techniques

The next step towards the setup of a numerical model is the discretization phase, which involves the spatial discretization and the equation discretization.

The spatial discretization consists in defining a grid or mesh that would represent the space continuum with a finite number of points where the numerical values of the physical variables must be determined. In Section 5.4.2.1-2, basic concepts for dealing with horizontal grids and vertical discretization will be introduced. Once the mesh is defined, we move to the final step related to the primitive equations discretization by using numerical methods, which consist in transforming the mathematical model into an algebraic, nonlinear system of equations for the mesh-related unknown quantities. The concepts on the basis of the time stepping are treated in Section 5.4.2.3. With the definition of the time-dependent numerical formulation, we finally select the discretization method to use for the equations, described in Section 5.4.2.4.

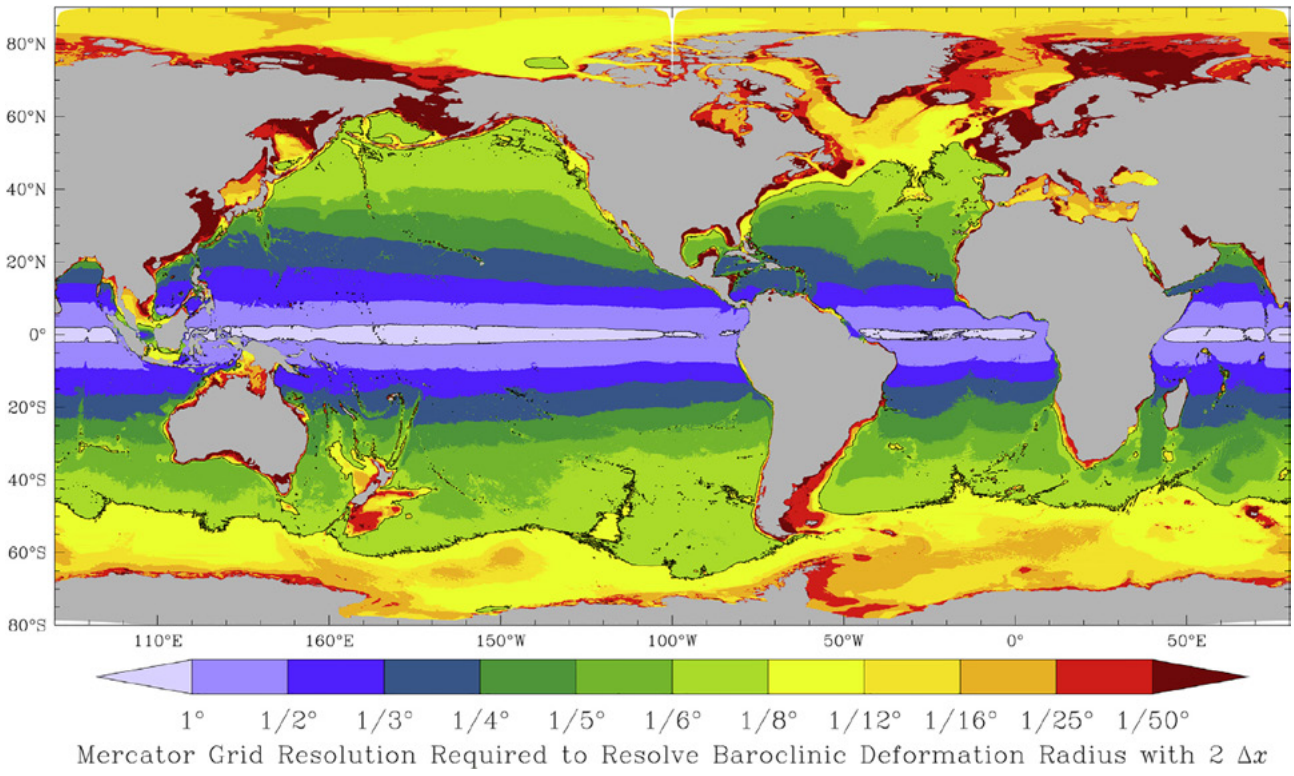

Figure 5.2. The horizontal resolution needed to resolve the first baroclinic deformation radius with two grid points, based on a 1/8º model on a Mercator grid on Jan 1 after one year of spinup from climatology (from Hallberg, 2013).

5.4.2.1. Horizontal grids

In numerical methods, we can use:

- Structured grids
- Unstructured grids

A mesh is structured when the grid cells have the same number of sides and the same number of neighbouring cells. Typically, in ocean models three kinds of grids may be used (Figure 5.3): the Arakawa-A grid, the Arakawa-B grid and the Arakawa C-grid. In the Arakawa-A grid (Figure 5.3A), all variables are evaluated at the same location. Then, the B and C grids have been developed respectively for coarse and fine resolution models. In the Arakawa-B grid (Figure 5.3B) both u (Northwards current component, in orange) and v (Eastwards current component, in green), for example, are evaluated at the same point and the velocity points are situated at the point that is equidistant from the four nearest elevation points (Elevation, in blue). In the Arakawa-C grid (Figure 5.3C), the u points lie east and west of elevation points, while the vpoints lie north and south of the elevation points .

Unstructured grids (Figure 5.4C) allow one to tile a domain using more general geometrical shapes (most commonly triangles) that are pieced together to optimally fit details of the geometry. They are extremely attractive for ocean modelling, especially for coastal models, in which the high-quality representation of geometrical features of a given domain is essential, and from the numerical point of view they may reach a significant level of complexity (Griffies et al., 2000).

Besides their ability to better represent coastlines, unstructured grid approaches also offer the possibility to smoothly increase the resolution over a region of interest or depending on physical parameters (Sein et al., 2017). This is also possible with structured curvilinear grids (for example, see the BLUElink Australian prediction model grid in Brassington et al., 2005, and Figure 5.4A), though with likely more constraints on the grid deformation properties. However, in any of the two cases, numerical stability is dictated by the smallest grid element, which substantially increases the computational problem. An additional difficulty is that sub-grid parameterizations have to be valid throughout the domain, whatever the grid size and eddy resolution regime are (Hallberg, 2013). In the structured grid case, block structured refinement techniques enable to circumvent some of the aforementioned difficulties by allowing a stepwise change (over a given grid patch) of the space and time resolutions (by integer factors, Figure 5.5B). Parameterizations and numerical schemes can also be changed accordingly. Grid exchanges can either be “one-way” if finer grids only receive information at their dynamical boundaries from the outer grid, or “two-way” if they also feed information back to the underlying mesh. In the latter case, data transferred at each model time step allows for a nearly seamless transition at the interface and possibly guarantees perfect conservation of prognostic quantities (Debreu et al., 2012).

Several libraries do facilitate the implementation of block structured refinement. Among them, the AGRIF library (Debreu et al., 2008) has been successfully used in HYCOM, MARS, NEMO and ROMS models. It is noteworthy that refinement techniques can eventually be adaptive, hence refinement regions can move

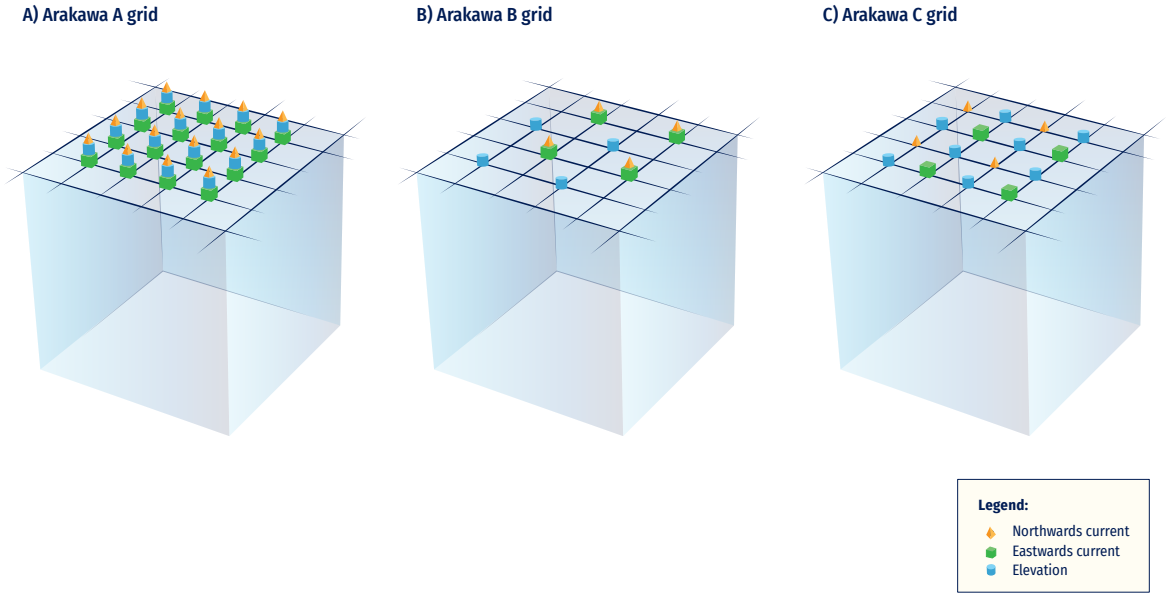

Figure 5.3. The three Arakawa types of grids (adapted from Dyke, 2016).

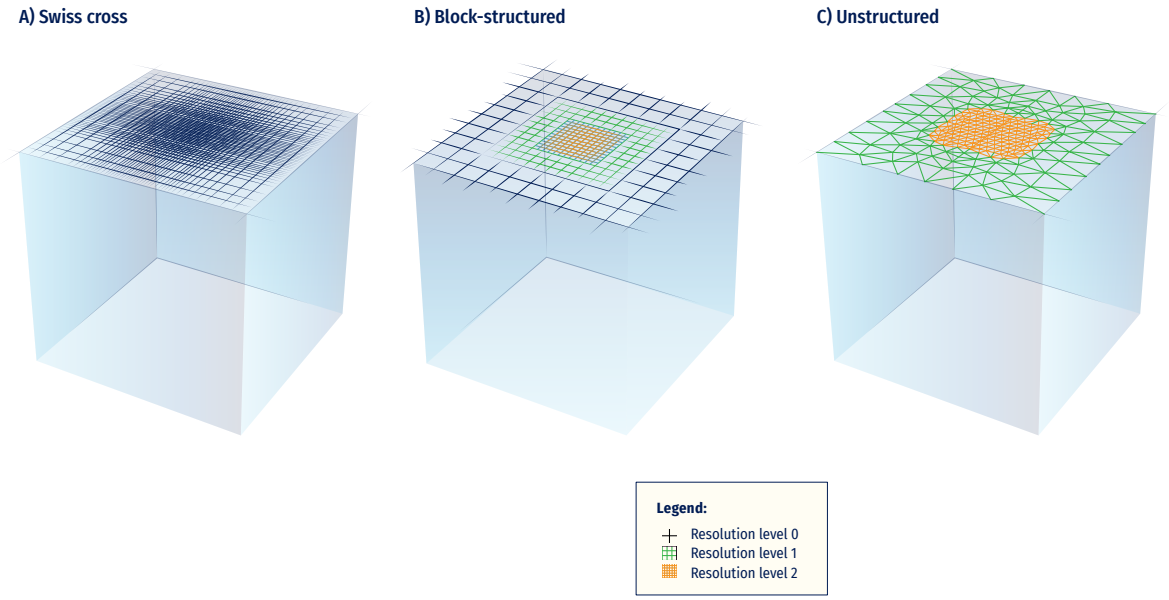

Figure 5.4. Possible ways to get a local increase of resolution: a) Progressive deformation of a structured grid; b) Block structured refinement; and c) Stretching of unstructured grid cells (adapted from Gerya, 2019).

over the course of the model integration (Blayo and Debreu, 1999). Resolution is in that case increased only where needed, depending on a local numerical or physical criterion, to save computing resources. The use of AMR techniques in realistic ocean models is nevertheless still poorly documented.

5.4.2.2. Vertical discretization

The problem of vertical discretization is connected to physical processes that the modeler wants to resolve and it must address questions related to: a) the representation of pressure gradients; b) the representation of sub-grid scale processes; c) the need to concentrate the resolution in a specific region (e.g. the shelf, the coastal areas, etc.); and d) the comparison with observations. Griffies et al. (2000) distinguished among three traditional approaches (Figure 5.5):

- Depth/geopotential vertical coordinates;
- Terrain-following;
- Potential density (isopycnic) vertical coordinates.

Geopotential (z-) coordinates (Figure 5.5A) have been largely used in ocean and atmospheric models because of their simplicity and straightforward nature for parameterizing the surface boundary layer. On the contrary, they are not able to adequately represent the effect of topography on the large-scale ocean models. Terrain-following coordinate systems (Figure 5.5B) are used especially in coastal applications, where bottom boundary layers and topography need to be well resolved. As z-coordinates, they suffer from spurious diapycnal mixing due to problems with numerical advection. In isopycnic vertical coordinates (Figure 5.5C), the potential density is referred to a given pressure. This system basically divides the water column into distinct homogeneous layers, which thicknesses can vary from place to place and from one time step to the next. This choice of coordinate works well for modelling tracer transport, which tends to be along surfaces of constant density. While both layered and isopycnal models use density as the vertical coordinate, there are subtle differences between the two types. Griffies et. al. (2000) and Chassignet et al. (2006), provide a discussion on the advantages and disadvantages of each vertical coordinate system.

5.4.2.3. Time stepping

Once the model is set from the spatial point of view and discretization in horizontal and vertical is defined, the time step for the computation needs to be considered as well. In the numerical schemes used to integrate the primitive equations, the time step must be small enough to guarantee computational stability. The Courant-Friedrichs-Lewy criterion (CFL) is the stability condition that states that the velocity c at which the information is propagating at times the time step Δt must be less than the horizontal grid spacing Δx:

$$C = \frac{u\Delta t}{\Delta x} \leq C_{max} \tag{5.8}$$

where C is the Courant number and C_{max} depends on the specific used scheme: explicit schemes allow to advance the solution to the next time level, one spatial grid point at a time, and are quite simple to implement (Kantha and Clayson, 2000);

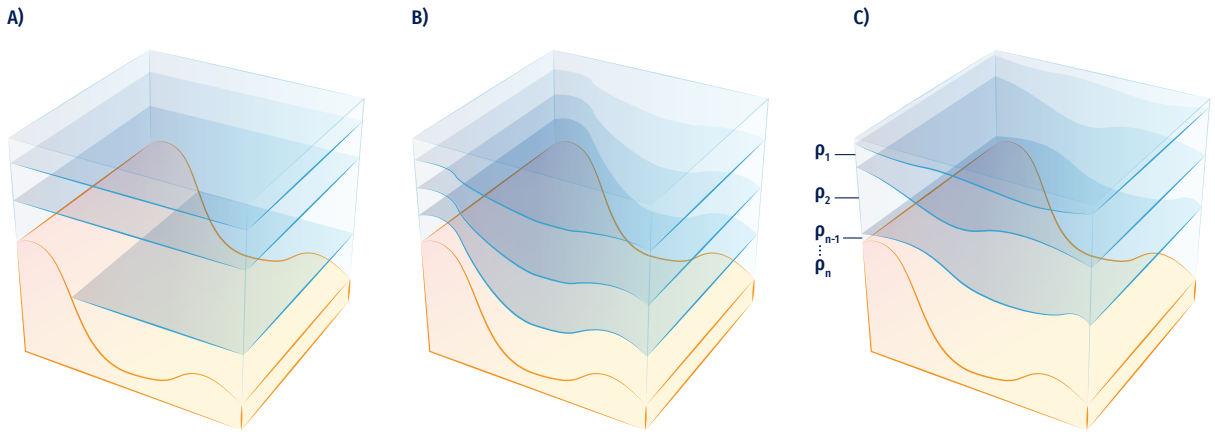

Figure 5.5. Vertical grid types: a) depth/geopotential vertical coordinates; b) terrain-following; and c) potential density (isopycnic) vertical coordinates.

in an implicit time-stepping scheme, the solution at the next time level must be derived for all grid points simultaneously. These schemes are computationally more intensive, but are unconditionally stable, thus permitting larger time steps to be taken than would otherwise be required.

5.4.2.4.Numerical techniques

Three families of methods are available for discretizing the space derivatives that enters in the primitive equations:

- Finite difference Method (FDM);
- Finite Volume Method (FVM);
- Finite Elements Method (FEM).

Here we provide an introduction to each method but for more detailed explanation refer to Hirsch, 2007.

The FDM is based on the properties of the Taylor expansions: it corresponds to an estimation of a derivative by the ratio of two differences according to the theoretical definition of the derivative, like the following:

$$u_x = \frac{\partial u}{\partial x} = \frac{u(x+\Delta x) - u(x)}{\Delta x} \tag{5.9}$$

If we remove the limit in Eq. 5.9, we obtain a finite difference: additionally, if Δx is "small" but finite, the expression on the RHS of Eq. 5.9 is an approximation of the exact value of u_x. Since Δx is finite, an error is introduced, called truncation error, which goes to zero for Δx tending to zero. The power of Δx with which this error tends to zero, is caller order of accuracy of the difference approximation and can be obtained by a Taylor series of $u(x+\Delta x)$ around point x (Eqq. 5.10 and 5.11):

$$u(x+\Delta x) = u(x) + \Delta \frac{\partial u}{\partial x} + \frac{\Delta x^2}{2}\frac{\partial^2 u}{\partial x^2} + \frac{\Delta x^3}{3!}\frac{\partial^3 u}{\partial x^3} + \dots \tag{5.10}$$

$$\frac{u(x+\Delta x)}{\Delta x} = \frac{\partial u}{\partial x} + \frac{\Delta x}{2}\frac{\partial^2 u}{\partial x^2} + \frac{\Delta x^2}{6}\frac{\partial^3 u}{\partial x^3} + \dots \tag{5.11}$$

Equation 5.11 shows that:

- The RHS of Eq. 5.9 is an approximation of the first derivative u_x in the point x;
- The remaining terms in the RHS represent the error associated with this formula.

If we restrict the truncation error to its dominant term, that is the lower power of Δx, we see that this approximation for $u(x)$ goes to zero like the first power of Δx and is said to be the first order in Δx:

$$\frac{u(x+\Delta x)}{\Delta x} \cong \frac{\partial u}{\partial x} + \frac{\Delta x}{2}\frac{\partial^2 u}{\partial x^2} = u_x(x) + O(\Delta x) \tag{5.12}$$

where $O(\Delta x)$ is the truncation error.

The FVM is a numerical technique by which the integral formulation of the conservation laws is discretized directly in the physical space. It is based on cell-averaged values, which makes this method totally different from FDM and FEM where the main numerical quantities are the local function values at the mesh points. For each cell, a local finite volume, also called control volume, is associated to each mesh point and applies the integral conservation law to this local volume. For this reason, the FVM is considered a conservative method. The essential property of this formulation is the presence of the surface integral and the fact that the time variation of a generic variable u inside the volume only depends on the surface values of the fluxes.

The FVM requires:

- The subdivision of the mesh, obtained from the space discretization, into finite small volumes, one control volume being associated to each mesh point;
- The application of the integral conservation law to each of these finite volumes.

The FEM originates from the field of structural analysis and it has two common points with the FVM:

- The space discretization is considered a set of volumes or cells, called elements;
- It requires an integral formulation as a starting point that can be considered as a generalisation of the FVM.

The FEM requires:

- Discretization of the spatial domain into a set of elements of arbitrary shapes;
- In each element, a parametric representation of the unknown variables, based on families for interpolating or shape functions, associated to each element or cell is defined.

Model	Grid topology	Numerical methods	Nesting capabilities	Website
NEMO	Structured grid	Finite Difference	Yes, with AGRIF	https://www.nemo-ocean.eu/
HYCOM	Structured grid	Finite Volume	Yes, with AGRIF	https://www.hycom.org/
MITgcm	Structured grid	Finite Difference	Yes	https://mitgcm.org/
ROMS	Structured grid	Finite Volume	Yes, with AGRIF	https://www.myroms.org/
CROCO	Structured grid	Finite Difference	Yes, with AGRIF	https://www.croco-ocean.org/
FVCOM	Unstructured grid	Finite Volume	Yes, with AGRIF	http://fvcom.smast.umassd.edu/
SHYFEM	Unstructured grid	Finite Element		https://sites.google.com/site/shyfem/project-definition
SCHISM	Unstructured grid	Finite Element		http://ccrm.vims.edu/schism-web/
FESOM	Unstructured grid	Finite Element		https://fesom.de/
MPAS	Unstructured grid	Finite Element		https://mpas-dev.github.io/
MOM	Structured grid	Finite Volume		https://www.gfdl.noaa.gov/ocean-model

Table 5.1. List of available ocean models used from global to coastal scales.

Such nice properties of the FEM as conservation of energy, that is common for all variational methods of solving differential equations, treatment of boundary conditions, and flexibility of irregular meshes have made them quite attractive, since they are also well suited to parallel computing. For this reason, it is considered as an interesting alternative to FDM commonly used in ocean modelling (Danilov et al., 2004).

5.4.3. List of Ocean General Circulation Models

In Table 5.1, are summarised some of the most used ocean models that integrate numerically the primitive equations for a wide range of spatial domains, from global ocean to coastal scales.

5.4.4. Downscaling large-scale solutions to regional/coastal circulation models

The need to resolve the small scales of ocean circulation in coastal seas, as well as the impracticability to run models at sufficiently high resolution and detailed physics at global scales, led to the development of downscaling approaches for both the direct modelling and the data assimilation problems.

Two families of modelling approaches can be distinguished: (1) models running at global scales with mesh refinement in the coastal areas of interest; and (2) one-way or two-way nesting of coastal models into regional or global ones. In practice, the first one is achieved by setting variable-mesh grids, such as unstructured or curvilinear structured grids (as discussed in 5.4.2.1). To our knowledge, only 2D (i.e. barotropic) unstructured models dedicated to storm surges and/or tides modelling, such as the tidal atlas FES2014 (Lyard et al., 2021), are running over the global ocean and satisfy the resolution requirements in shallow waters. In the second approach, the large-scale global (or regional) model, i.e. the 'parent' model, provides open-boundary conditions to the coastal ('child') model; in case of two-way nesting, both models are coupled and the child model returns an estimate of the ocean state at its boundary, which is used in turn to

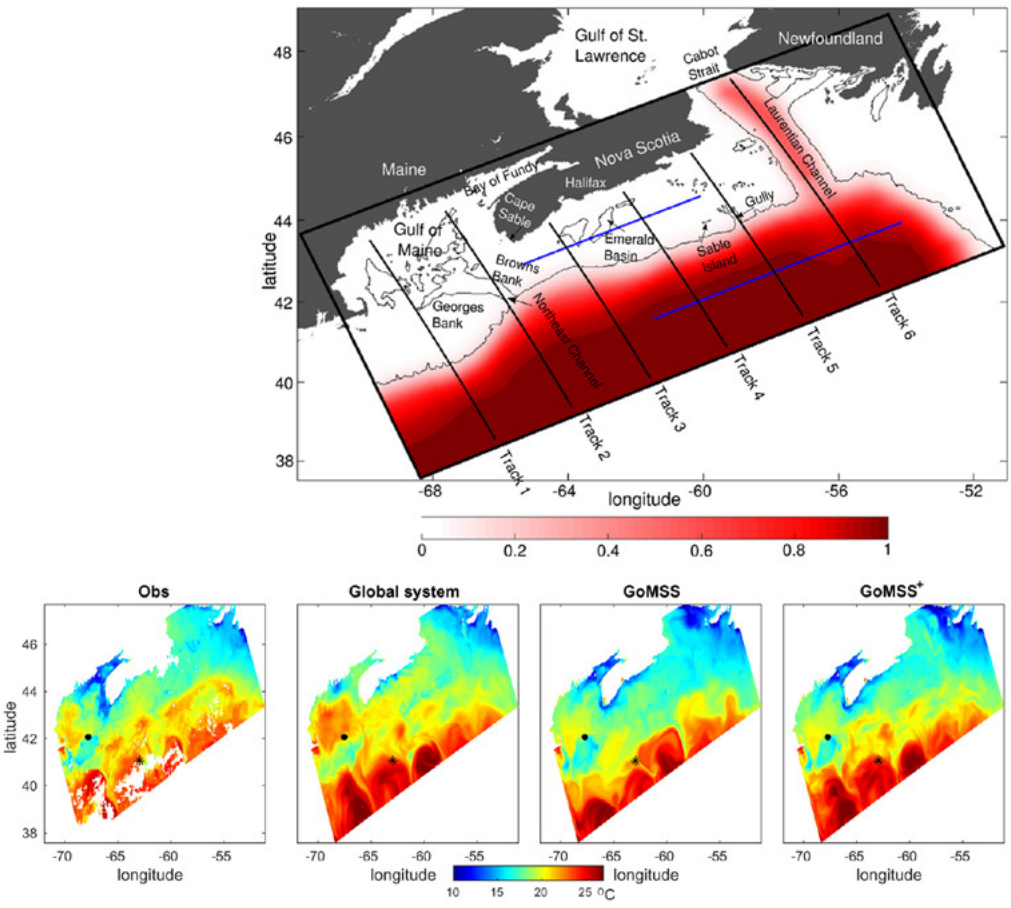

Figure 5.6. Spectral nudging in the Gulf of Maine; top: spatial domain; bottom: snapshots of sea surface temperature on 22 Jul 2012 from observations, global system, regional configuration and regional configuration with spectral nudging (from Katavouta and Thompson, 2016).

force the parent simulation. General resolution issues for both approaches and practical considerations are discussed in Greenberg et al. (2007).

However, nesting methods do not just consist in reproducing the large-scale solution with more details. Indeed, the child model may represent different processes from those solved by the parent model (e.g. tides, surface gravity waves, etc.) or may rely on different parameterizations or parameters. Besides, due to the strong nonlinearity of the ocean flow, the internal variability of the child model may decouple from that of the parent, leading to divergent solutions (Katavouta and Thompson, 2016). Figure 5.6 shows an example of spectral nudging in the Gulf of Maine as in Katavouta and Thompson (2016). The spatial domain is given in Figure 5.6-top: the black box represents the bounding box of the regional model GoMSS (NEMO, 1/36° horizontal resolution), which is nested into the HYCOM+NCODA global 1/12° analysis system. GoMSS+ is the regional configuration with spectral nudging where temperature and salinity variables are directly updated. By adopting such a nesting approach, the regional configuration significantly improves the quality of the solution as shown in Figure 5.6-bottom: it represents the sea surface temperature snapshots for 22 July 2012 based on satellite ("Obs"), the global system ("Global system"), the regional system ("GoMSS"), and that implementing the spectral nudging ("GoMSS+"). The GoMSS+ exhibits an improved version of the coastal sea surface temperature representation, which is typical for a higher resolution model that takes into account coastal processes (e.g., tides). At the same time, it is able to capture the warm slope water and cold shelf waters as shown in the observations, which are well represented in the global model thanks to data assimilation. For further details, please refer to Katavouta and Thompson (2016).

In 2007, the GODAE Coastal and Shelf seas Working Group (De Mey et al., 2007) noted that: "It is becoming increasingly clear that specifying the offshore boundary conditions of coastal models by using forecasts from a hydrodynamical large-scale ocean model has the potential (1) to provide better local estimates by adding value to GODAE products, (2) to extend predictability on shelves, and (3) to enhance the representativeness of local observations." Despite considerable efforts since 2007 on both coastal modelling capabilities and nesting methods, downscaling still raises obvious numerical and physical issues. In the following paragraphs an attempt has been made, but not exhaustively, to present the various difficulties that arise and the solutions found in the literature to address them.

The coastal ocean is subject to both local (e.g. atmosphere, river mouths) and remote forcings (e.g. astronomical potential, coastal waveguide, wind fetch, biogeochemical connectivity). Therefore, the boundaries of a coastal model, which also intercept strong bathymetry gradients, play a critical role. In addition, solving primitive equations on a limited area domain with OBC does not lead to a unique physically realistic solution. Consequently, a variety of ad hoc methods to set-up practical OBC have been developed with a dependence upon flow dynamics, model resolution, types of information at the open boundaries, etc., as reviewed by Blayo and Debreu (2005). A simple view of the OBC issues consists in viewing the problem because of inconsistencies between the parent and child models which, as mentioned previously, arise due to different physics of the model, to different forcing (e.g. atmospheric, runoff, bathymetry), and to truncated information at the open boundary. The last refers to the fact that the parent information is provided as discrete fields in space and time (e.g. daily or hourly averages); high-frequency motions are therefore filtered out or aliased.

The example of tides is particularly enlightening on these limitations. Even though the parent model resolves tides, forcing the child with the parent tidal waves (either barotropic or both barotropic and baroclinic) implies the availability of the large-scale forcing at very high frequency (a few minutes). In practice, especially for operational systems, this is very difficult to achieve as it requires huge storage capacities. Therefore, coastal models are usually forced by low-frequency dynamics and tidal constituents, both of which not necessarily stemming from the same parent models (tidal constituents are often chosen from accurate global tidal atlases). Herzfeld and Gillibrand (2015) noted that conditions for incoming tidal waves may be reflective for the low-frequency external data and propose OBC based on dual relaxation time scales. Furthermore, the difference of bathymetry and representation of the coastline between the parent and child models may lead to large inconsistencies between the tidal solutions in both models, with a risk of spurious patterns developing in the coastal domain close to the open boundaries (e.g. rim currents). Toublanc et al. (2018) proposed a simple approach that reduces such inconsistencies by pre-processing the tidal forcing using a 2D simulation with a dedicated 2D tidal model. At last, filtering out the high-frequency 3D incoming information by using for instance hourly or daily averages from the parent simulation, may lead to a loss of energy in the coastal domain, in particular because of the missing internal waves forcing, as recently evidenced by Mazloff et al. (2020).

Another difficulty in one-way nesting arises from the possibility that the child model develops an internal variability that diverges from the parent's one. In many operational systems, global or large-scale solutions stem from a data assimilation system in which the mesoscale dynamics are constrained by satellite data (e.g. altimetry). If no data assimilation is performed in the coastal domain, the developing mesoscale (and a fortiori submesoscale) may deviate from reality leading to the undesirable case in which the parent solution is closer

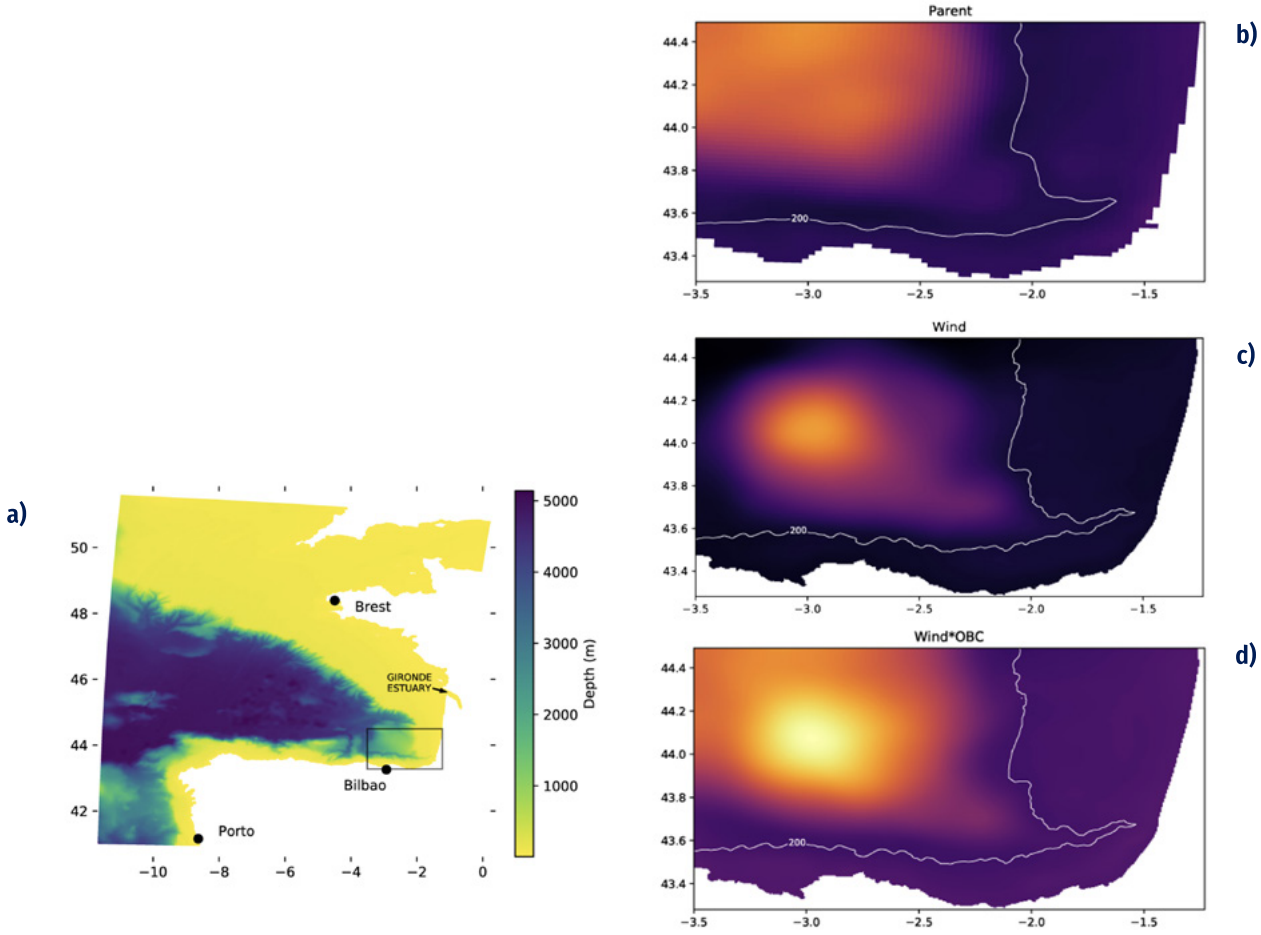

Figure 5.7. A case study in the south-east Bay of Biscay: a) bathymetry of the parent model and bounding box (black box) of the child domain; ensemble spread in SSH over 3 months period (Jan-Feb-Mar) from 50 ensemble members perturbing; b) wind in parent model; c) wind in the child domain; and d) wind and OBC in the child domain (from Ghantous et al., 2020).

to observations at large-scale and mesoscale than the child. Sandery and Sakov (2017) report that even with data assimilation, increasing the resolution does not automatically improve the skill of the forecast, because of the inverse cascade of unconstrained submesoscale towards mesoscale. Methods such as spectral nudging are developed to ensure that the large-scale patterns, e.g. eddies or meandering jets that are accurately represented in the parent model, are maintained in the child; an example of such method can be found in Katavouta and Thompson (2016).

A last but not least issue concerns quantifying the errors in the child simulations due to the nesting process. The errors originate from the OBC scheme (numerical implementation and physical assumptions) and from the uncertainties on the parent forcing fields. In the latter case, the question is how the parent model errors are downscaled. Ensemble approaches can help to characterise and estimate the downscaling of parent errors, as for instance explored in Ghantous et al. (2020).

Figure 5.7 shows an example of ensemble downscaling of a coastal ocean model (Symphonie model, 500 m resolution) for the south-east Bay of Biscay in an ensemble of a regional model (NEMO, 1/36°) (Ghantous et al., 2020). Figure 5.7a presents the regional domain, in particular the parent domain over the map, while the blue box is the domain of the child model. Figures 5.7b-d show the ensemble spread (standard-deviation) in sea surface height (SSH) in the domain of the child model for ensembles of 50 members. In particular, Figure 5.7b is the parent ensemble, generated by perturbing the wind in the parent domain; Figure 5.7c is the child ensemble, generated by perturbing the wind in the child domain; Figure 5.7d is the child ensemble generated by perturbing both the wind and the OBC conditions (the OBC perturbations stem from the parent ensemble). The numerical experiment reveals that, on average over the period of study, the spread in SSH is greatest where the mesoscale eddies are present (in the deeper area of the domain). It also reveals that the contribution from the OBC uncertainties is larger than the impact

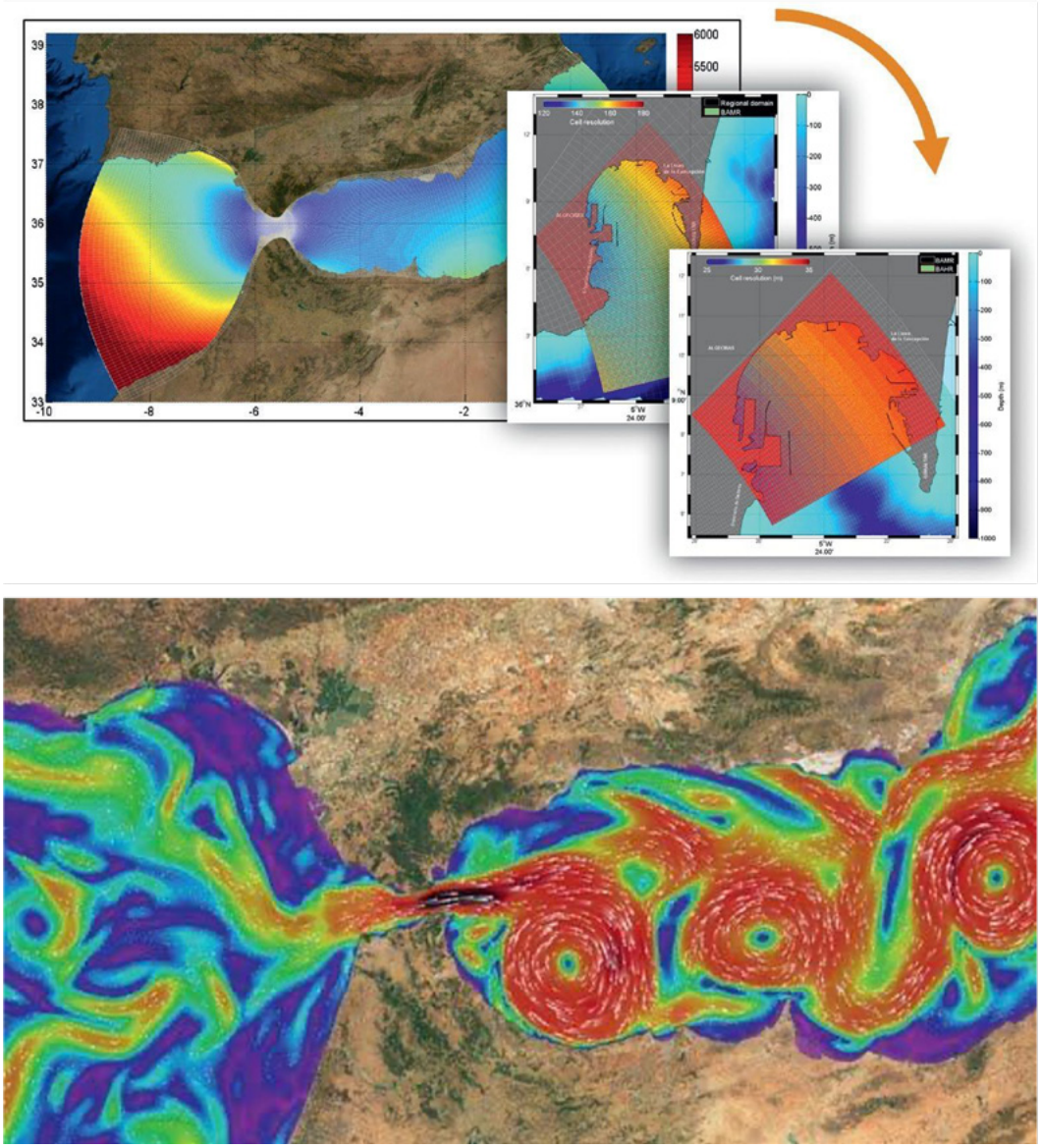

Figure 5.8. Gulf of Cadiz and the Alborán Sea: example of downscaling capacities. Source: Puertos del Estado and Universidad de Málaga.

of local wind uncertainties. It is a valuable result for the next generation of ensemble data assimilation systems.

An example of nesting capacities of circulation modelling in short-term forecast is shown in Figure 5.8. This is the result of downscaling the Copernicus Marine Service Iberia-Biscay-Ireland – Monitoring and Forecasting Centre (IBI-MFC, [1]) product on a higher spatial grid; in the bottom panel it can be seen a detail of surface currents in the Gulf of Cadiz and Alborán Sea.

The downscaling approach is extremely powerful to allow the modeller to set up an OOFS at high resolution, and every OOFS may be used to build another OOFS in a seamless way. In Section 5.9 can be found an initial but exhaustive list of OOFSs' providers from which the modeller may select to nest her/his new OOFS.

1. https://resources.marine.copernicus.eu/product-detail/IBI_ANALYSISFORECAST_PHY_005_001/INFORMATION

5.5. Data assimilation systems

An introduction to the data assimilation concept can be found in Section 4.3. This Section focuses on the numerical characteristics of the DAS largely used in circulation modelling.

5.5.1. Basic concepts

In ocean forecasting the objective is to produce an estimate x_a of the true state x_t of the ocean at initial time to initialise forecasts. Ide et al., 1997, De Mey-Frémaux et al. (1998), and Bouttier and Courtier (2002) provide an extensive introduction to DAS basic concepts and herein are recalled and summarised.

DA consists in calculating the «best» estimate of the state of a physical system, of its evolution in time, given observations and a prognostic numerical model.

The basic objective information that can be used to produce the analysis is a collection of observed values provided by observations of the true state. If the model state is overdetermined by the observations, then the analysis is reduced to an interpolation problem. In most cases the analysis problem is under-determined because data are sparse and only indirectly related to the model variables. In order to make it a well-posed problem, it is necessary to rely on some background information in the form of an a priori estimate of the model state.

A discrete model for the evolution of the ocean from t_i to t_{i+1} is governed by the following Eq. 5.13:

$$\mathbf{x}^f(t_{i+1}) = M_i\left[\mathbf{x}^f(t_i)\right] \tag{5.13}$$

where $\mathbf{x}$ is the so-called state vector (velocities, temperature, salinity, etc., at model grid positions) and M is the corresponding dynamics operator. The state vector has dimension n. The dynamic operator in Eq. 5.13 is commonly non linear and deterministic, while the true ocean state may differ from Eq. 5.13 by random and systematic error.

Observations y_t^o at time t_i are defined by Eq. 5.14:

$$\mathbf{y}_t^o = H_i\left[\mathbf{x}^t(t_i)\right] + \epsilon_i \tag{5.14}$$

where H is an observation operator and ϵ is a noise process. The observation vector has dimension p_i. A major problem of data assimilation is that typically p_i<<n. The observation operator H can be also non-linear like M and both can contain explicit time dependence in addition to the implicit dependence via the state vector $\mathrm{x}^f{}_i \equiv x^f(t_i)$. The noise process ϵ is commonly used to have zero mean and we denote its covariance matrix by R: it consists of instrumental and representativeness errors which covariance matrices are E and F, respectively, with R=E+F.

The key of the analysis is the use of discrepancies between observations and state vector:

$$y^o - H(x) \tag{5.15}$$

When calculated with the background x_b it is called innovations and with the analysis x_a analysis residuals.

In the following, we present two data assimilation types of approaches: the sequential methods and the variational methods.

5.5.2. Sequential methods

Several schemes have been proven useful and implemented using a sequential-estimation approach including the Bluelink Ocean Data Assimilation System (BODAS) (Oke et al., 2008) and the Singular Evolutive Extended Kalman (SEEK) filter (Pham et al., 1998). An extensive literature is available on related methods, such as OI (Daley, 1991), EnOI, and EnKF (Evensen, 2003).

Following Ide et al., (1997), the true ocean fluid $\mathbf{x}^f$ is assumed to differ from that of the numerical model (Eq. 13) by stochastic perturbations:

$$\mathbf{x}^f(t_{i+1}) = M_i\left[\mathbf{x}^f(t_i)\right] + \eta(t_i) \tag{5.16}$$

where η is a noise process with zero mean and covariance matrix $\mathbf{Q}$. The EKF consists of a forecast step based on previously obtained state variables, which include previous assimilation steps, $\mathbf{x}^f(t_{i+1})$ and an updated probability function described by $\boldsymbol{P}^f(t_i)$:

$$\mathbf{x}^a(t_i) = M_i\left[\mathbf{x}^a(t_{i-1})\right] \tag{5.17}$$

$$\mathbf{P}^f(t_i) = \mathbf{M}_{i-1}\mathbf{P}^a(t_{i-1})\mathbf{M}_{i-1}^T + \mathbf{Q}(t_{i-1}) \tag{5.18}$$

The core of the Kalman Filter method is an update step in which the observations available at time i is blended with the previous information, taking account of their joint probability distributions and carried forward by the forecast step:

$$\mathbf{x}^a(t_i) = \mathbf{x}^f(t_i) + \mathbf{K}_i\mathbf{d}_i \tag{5.19}$$

$$\mathbf{P}^a(t_i) = (\mathbf{I} - \mathbf{K}_i\mathbf{H}_i)\mathbf{P}^f(t_i) \tag{5.20}$$

where the observation residual or innovation vector is defined by:

$$\mathbf{d}_i = \mathbf{y}_i^0 - H_i\left[\mathbf{x}^f(t_i)\right] \tag{5.21}$$

The Kalman gain $\mathbf{K}_i$ is defined by:

$$\mathbf{K}_i = \mathbf{P}^f(t_i)\mathbf{H}_i^T\left[\mathbf{H}_i\mathbf{P}^f(t_i)\mathbf{H}_{i-1}^T + \mathbf{R}_i\right]^{-1} \tag{5.22}$$

The innovation vector $\mathbf{d}_i$ is evidently a displacement of the modelled forecast toward the observed data, scaled by the Kalman gain. The Kalman gain accounts for the weighting required by the joint probability function for the model and observation variability. In practice, various simplifications are introduced to describe $\mathbf{P}$ to overcome the computational burden involved in the matrix calculation (Oke et al., 2008; Pham et al., 1998).

Another example is the *OI* that is quite frequently used in oceanography and meteorology. It is a particular suboptimal filter, in which the EKF's error covariance matrix P^f is replaced by an approximation, $\mathbf{B}$, computed as a product of variances placed in the diagonal matrix $\mathbf{D}$ and of correlations placed in a matrix $\mathbf{C}$ with unit diagonal (Ghil and Malanotte-Rizzoli, 1991):

$$\mathbf{B} = \mathbf{D}^{1/2}\mathbf{C}\mathbf{D}^{1/2} \tag{5.23}$$

The state vector is still given by Eq. 5.13. The *OI* gain writes:

$$\mathbf{K}_i^{OI} = \mathbf{B}^f(t_i)\mathbf{H}_i^T\left[\mathbf{H}_i\mathbf{B}^f(t_i)\mathbf{H}_i^T + \mathbf{R}_i)\right]^{-1} \tag{5.24}$$

where $\boldsymbol{H}_i\boldsymbol{B}^f(t_i)\mathbf{H}^T{}_i$ is evaluated from the correlation model, and the state update is given by:

$$\mathbf{x}^a(t_i) = \mathbf{x}^f(t_i) + \mathbf{K}_i^{OI}\mathbf{d}_i \tag{5.25}$$

5.5.3. Variational methods

Several schemes have been implemented using variational methods such as 3D-Var, e.g. the Navy Coupled Ocean Data Assimilation (NCODA) (Cummings, 2005) and the Forecasting Ocean Assimilation Model (FOAM) (Martin et al., 2007). 4D-Var methods are used extensively in Numerical Weather Prediction and are one of the future directions for ocean prediction systems. The NEMOVAR system (Mogensen et al., 2012) is able to handle both categories of variational approaches for the NEMO modelling system.

Following Ide et al. (1997), 4D-Var minimises the objective function *J* that measures the weighted sum of distance J^b to the background state $\mathbf{x}^b$ and J^o to the observation $\mathbf{y}^o$ distributed over a time interval $[t_0, t_n]$:

$$\begin{aligned} J\left[\mathbf{x}(t_0))\right] = &\frac{1}{2}\left[\mathbf{x}(t_0)) - x^b(t_0)\right]^T\mathbf{B}_0^{-1}\left[\mathbf{x}(t_0)) - \mathbf{x}^b(t_0)\right] \\ &+ \frac{1}{2}\sum_{i=0}^{N}\left[\mathbf{y}_i - \mathbf{y}_i^0\right]^T\mathbf{R}_i^{-1}\left[\mathbf{y}_i - \mathbf{y}_i^0\right] \end{aligned} \tag{5.26}$$

where $\mathrm{y}_i \equiv H_i[\mathrm{x}(t_i)]$. Here B^{-1} is an a priori weight matrix, with B meant to approximate the error covariance matrix x^b, and a minimization is done with respect to the initial state $x(t_0)$.

Equation 5.25 reflects the imposition of a strong constraint (Sasaki, 1970). Alternative formulations based on a weak constraint are given by Bennett (1992) and by Menard and Daley (1996). Efficient methods for performing the minimization of *J* require its partial derivatives with respect to the elements of $\mathrm{x}(\mathrm{t}_0)$ given by:

$$\begin{aligned} \left[\frac{\partial J}{\partial x(t_0)}\right] = &\mathbf{B}_0^{-1}\left[\mathbf{x}(t_0) - \mathbf{x}^b(t_0)\right] \\ &+ \sum_{i=0}^{N}\mathbf{M}(t_{i+1}, t_0)^T\mathbf{H}_i^T\mathbf{R}_i^{-1}(\mathbf{y}_i - \mathbf{y}_i^0) \end{aligned} \tag{5.27}$$

where:

$$\mathbf{M}(t_i, t_0)^T = \Pi_{j=0}^{i-1}\mathbf{M}(t_{j+1}, t_j)^T \tag{5.28}$$

This follows from:

$$\left[\frac{\partial J}{\partial \mathbf{x}_{i+1}^f}\right]^T = \mathbf{M}(t_{i+1}, t_i)^T\left[\frac{\partial J}{\partial \mathbf{x}_i^f}\right]^T \tag{5.29}$$

$$\left[\frac{\partial J}{\partial \mathbf{x}_i}\right]^T = \mathbf{H}_i^T\left[\frac{\partial J}{\partial \mathbf{y}_i}\right]^T \tag{5.30}$$

$\mathbf{M}(t_{i+1}, t_i)^T$ is usually called adjoint model and $\mathbf{H}^T{}_i$ is the adjoint observation operator. 4D-Var reduces to three-dimensional variational assimilation (3D-Var) if the time dimension is taken out.

Figure 5.9 shows an example of 4D-Var capacity: x_a is used as the initial state for a forecast, then by construction of 4D-Var one is sure that the forecast will be completely consistent with the model equations and the 4D distribution of observations until the end of the 4D-Var time interval *n* (the cutoff time).

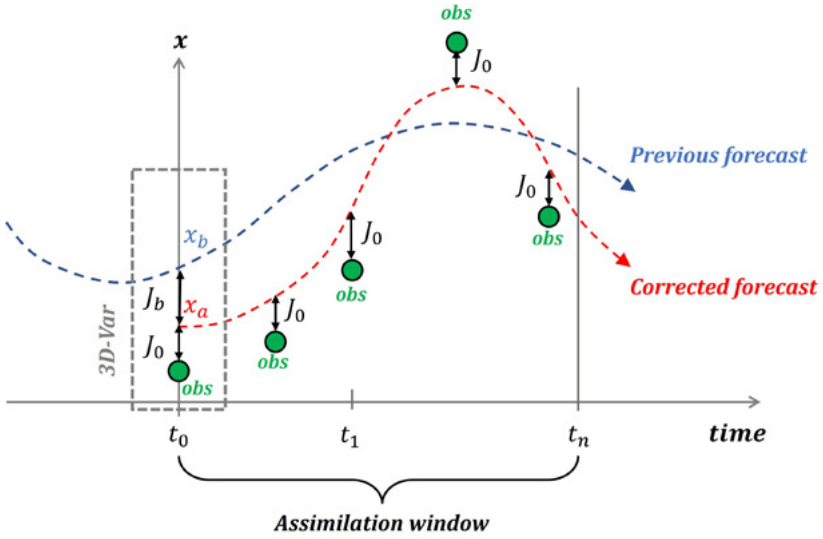

Figure 5.9. Example of 4D-Var intermittent assimilation in a numerical forecasting system (adapted from Bouttier and Courtier 2002).

5.5.4. Modelling errors

As reported in Bouttier and Courtier (2002), to represent the fact that there is some uncertainty in the background and in the analysis, we need to assume some model of the errors between these vectors.

Given a background field $\mathbf{x}_b$ just before doing an analysis, we define the vector of errors that separates it from the true state:

$$\epsilon_b = \mathbf{x}_b - \mathbf{x}_t \tag{5.31}$$

If we are able to repeat each analysis experiment a large number of times, under exactly same conditions but with different realisation of errors generated by unknown causes, b would be different every time. It can be represented through a probability density function (PDF), able to provide all statistics, including the average (or expectation) -b and the variances. A popular model of scalar pdf is the Gaussian function, that can be generalised to a multivariate PDF.

The errors in the background and in the observations are modelled as follows:

- Background errors. They are the estimation errors of the background state, given by the difference between the background state vector and its true value;
- Observation errors. They contain errors in the observation process (i.e instrumental errors), errors in the design of the operator *H*, and representativeness errors (i.e. discretization errors which prevent x^t from being a perfect image of the true state;
- Analysis error. Defined through the trace of the covariance matrix $\mathbf{A}$:

$$Tr(\mathbf{A}) = \overline{\| \epsilon_a - \bar{\epsilon_a} \|^2} \tag{5.32}$$

They are the estimation errors of the analysis state, which is what we want to minimize. In a scalar system, the background error covariance is the variance:

$$\mathbf{B} = var(\epsilon_b) = var\overline{| \epsilon_b - \bar{\epsilon_b} |^2} \tag{5.33}$$

In a multidimensional system, B is a square symmetric matrix with n×n dimension. The diagonal of B contains the variances, while the off-diagonal contains the cross-covariances between a pair of variables in the model. The off-diagonal terms can be transformed into error correlations:

$$\rho(e_i, e_j) = \frac{cov(e_i, e_j)}{\sqrt{var(e_i)var(e_j)}} \tag{5.34}$$

The error statistics are functions of the physical processes governing the meteorological or the ocean state and the observing network. They depend on a priori knowledge of the errors: variances reflect our uncertainty in features of the background or the observations. To estimate statistics, it is necessary to assume that they are stationary over a period and uniform over a domain, so that one can take a number of error realisations and make empirical statistics.

In setting a DAS, the estimated statistics is very difficult and we can rely on diagnostics of an existing data assimilation system using the observational method.

5.5.5. Overview of current data assimilation systems in operational forecasting

Data assimilation techniques, schematically introduced in previous paragraphs and that are widely documented in Daley (1991), Evensen (2003) and Zaron (2011), represent the baseline of the modelling framework with general circulation models for operational forecasting and reanalysis. At international level, the GODAE's OceanView (Bell et al., 2015) and OceanPredict initiatives have promoted strong synergies with GOOS, ETOOFS and GEO BluePlanet contributing to a value chain from observations, data, information systems, predictions, and scientific assessments to end users, with the aim to promote the use and impact of observations and ocean predictions for societal benefit, and increasing visibility of operational oceanography advances.

Martin et al. (2015) presents an overview of the main characteristics of the data assimilation used in each GODAE OceanView systems; this is a list of the adopted numerical techniques:

- Bluelink (Oke et al., 2013) adopts MOM4 ocean model and EnOI algorithm;
- GIOPS (Smith et al., 2016) uses NEMO ocean model and SEEK (with fixed basis) for the ocean component, and 3DVar for assimilation in the ice component;
- ECMWF (Balmaseda et al., 2013) uses NEMO ocean model and 3DVar for the assimilation component (+ bias correction technique);
- FOAM (Waters et al., 2014) uses NEMO ocean model and 3DVar for the assimilation component (+ bias correction technique);
- GOFS (Cummings and Smedstad, 2013) uses HYCOM ocean model with 3DVar data assimilation scheme;
- Mercator Ocean (Lellouche et al., 2013) uses NEMO ocean model with SEEK-FGAT (with fixed basis) and 3DVar bias correction;
- MOVE (Usui et al., 2006) uses MRI COM model and 3DVar data assimilation scheme;
- TOPAZ (Sakov et al., 2012) uses HYCOM with EnKF techniques.

Description of the operational initiatives is also provided at GODAE OceanView website ([2]) and OceanPredict website ([3]).

5.6. Ensemble modelling

Numerical models, applied to nonlinear dynamical systems such as the ocean, inevitably approximate the solution of the so-called Navier-Stokes shallow-water equations, because of limitations in computer power to resolve the whole spectrum of geophysical processes. In addition, numerical modelling is subject to numerous inherent uncertainties related to modelling parameters, to forcing functions, to initial and boundary conditions. This is why a single forecast is, to some extent, uncertain, and we use ensemble modelling to answer how uncertain a forecast is. Ensemble prediction systems (EPS) are well-known in atmospheric science communities for more than 25 years (Palmer, 2018) but are more recent in operational oceanography, with marked advances in the last decade (e.g., TOPAZ system, Sakov et al., 2012). EPS uses ensemble modelling and adds other components, such as probabilistic outputs and soon machine learning under varying flavours, with prediction as objective. In most cases, EPS also incorporates ensemble-based data assimilation (DA) to decrease forecast errors.

Due to the chaotic nature of the ocean, the probabilistic approach is an interesting alternative beyond the classic deterministic approach, and it can help users to interpret model predictions supplemented by their uncertainties. Ensemble modelling consists of possible ocean states using Monte Carlo techniques to sample the probability density function (pdf) of the model forecast. Each model simulation is called an ensemble member. This approach is illustrated in Figure 5.10a. The ensemble is initialised by a sample of different initial conditions (e.g. perturbed analyses in DA). The model operator (which can be also perturbed during integration) is then used to bring forward in time each member and produce an ensemble of model simulations. The ensemble members may diverge radically or remain broadly similar, resulting in a forecast PDF. A quantitative assessment of the ensemble is depicted in Figure 5.10b. The ensemble mean and spread (estimating model uncertainty) are calculated as first and second order statistical moments from the members, and can be compared with the unperturbed deterministic simulation and the climatology (and to observations, if available). The ensemble spread is flow-dependent

2. https://www.godae-oceanview.org/
3. http://oceanpredict19.org

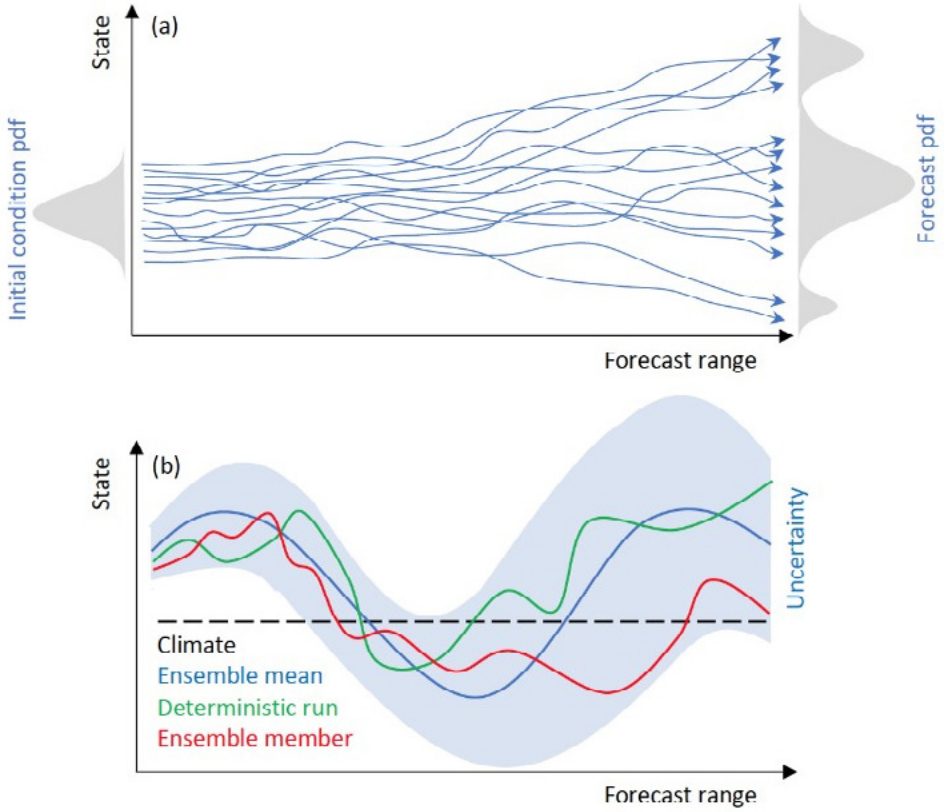

Figure 5.10. (a) Schematic of an ensemble simulation with equiprobable forecasts (blue trajectories); the forecast pdf gives an indication of the likelihood of occurrence of the different states; (b) Schematic of the flow-dependent ensemble spread in relation to the ensemble mean, an individual member, the unperturbed deterministic run, and the climatology (credits: [4]).

and varies for different state variables. Ensemble forecasting aims at quantifying this flow-dependent uncertainty. EPS are highly demanding systems in terms of computational resources and can be run efficiently in HPC facilities. A major challenge for the next generation of OOFSs is to improve their services by integrating ensemble capabilities in their systems.

5.6.1. Basic concepts

There are three main categories of ocean model ensembles: (a) multi-model ensembles, e.g. Copernicus Marine Service multi-model products and CMIP6 coupled models for climate studies ([5]); (b) stochastic model ensembles, used in research e.g. the OCCIPUT project (Penduff et al., 2014), and less frequently in operational oceanography due to their computational cost; and (c) ocean model response to an atmospheric EPS, e.g. using the ECMWF-EPS atmospheric forcing([6]).

The focus here is on the practical aspects for the implementation of a stochastic ocean model, mainly for short- to medium-range forecasting applications. The notion "stochastic model" for a system exhibiting chaotic behaviour can be defined by the partial differential Fokker-Planck equation, describing the temporal evolution of the state pdf, controlled by stochastic diffusion and advection processes, and local model tendencies. Stochastic modelling is used to represent model errors and as an ulterior step can be integrated in ensemble-based DA. Several methods and tools to produce stochastic model ensembles have been discussed in the literature following the SANGOMA project ([7]).

The main objectives of (ensemble) stochastic modelling are: (a) the estimation of model uncertainties providing realistic error bars and confidence intervals at useful ranges for ocean predictions; and (b) using model uncertainties in a DA framework to enrich background error covariances with flow-dependent errors and improve model prediction at the range of the outer loop of the DA scheme. The most useful

4.https://confluence.ecmwf.int/
5. https://www.wcrp-climate.org
6. https://www.ecmwf.int/en/forecasts

7. http://www.data-assimilation.net

statistical properties are the ensemble mean, the covariances and spread given by the diagonal of the covariance matrix, and sometimes the higher order moments (Quattrocchi et al., 2014). Stochastic ensembles are not used solely for DA but can be applied also as a machine learning base for artificial intelligence applications, guiding observational strategies based on array design (Charria et al., 2016; Lamouroux et al., 2016), and enabling probabilistic forecasting (Cheng et al., 2020), e.g. occurrence of ocean upwelling or bloom events, occurrence of sea level and storm surge exceeding a particular threshold, sea ice concentration, etc.

The main elements to be decided and identified when generating an ocean model ensemble are: (a) the relevant quantities to perturb; (b) the stochastic parameterizations; and (c) the dynamical balances that must be preserved, if any (which in turn influence choices in (a)). These notions are often combined under the term "stochastic physics".

The ensemble verification is an important integral part of the ensemble modelling and EPS-developing process. An ensemble empirical consistency aims at verifying a posteriori the model pdf approximated by the ensemble of forecasts, with respect to existing observations and their pdfs. The underlying notion is the model and data joint probability on the right-hand-side of the equal sign in the Bayes theorem. Empirical consistency can be explored by specific criteria and analysis tools, e.g. from rank histograms being the simplest measuring "reliability" (Candille and Talagrand, 2005) to Desroziers et al. (2005) consistency diagnostics on innovations and ensemble pattern-selective consistency analysis (Vervatis et al., 2021a). The "reliability" measures to which degree the forecast probabilities agree with outcome frequencies and is an important attribute for the development of probabilistic scores. Such scores are for example the Continuous Rank Probability Score (CRPS) (Hersbach, 2000; Candille and Talagrand, 2005) and the Brier Score measuring, in addition to "reliability", the attribute of "resolution". For a reliable EPS, "resolution" is the ability to separate cases when an event occurs or not, i.e. probabilities being close to 0 or 1. The ensemble consistency evaluation framework provides important information to test the relevance of an EPS when the system is set-up (e.g. the ensemble size).

5.6.2. Ocean model uncertainties

Ocean model uncertainties emerge from sources of errors relevant to the ocean state, including physics, biogeochemistry, and sea ice, as well as errors in the initial state and boundary conditions (i.e. atmospheric forcing and lateral open boundary conditions). Model uncertainties in ocean physics have a significant impact in all other system components as, for example, in biogeochemistry and sea ice. The choice of the perturbed model quantities depends: (a) on the ocean application, e.g. global vs regional and coastal configurations, and short- to medium- or seasonal-range forecasts; (b) on the processes resolved by the model (or not, such as sub-grid scale processes); (c) on choices in the DA framework, e.g. variational and Kalman filter approaches, variables and parameters included in the control vector, assimilated observations etc.; and (d) on the dynamical balances the user wants to preserve in the perturbation space, e.g. leaving velocities unperturbed tends to preserve the degree of geostrophy of the ocean state.

Recent advances in NEMO incorporated an easy-to-use modelling framework for the production of ocean model ensembles (Brankart et al., 2015), including the following schemes applied also in NWP systems: SPPT (Buizza et al., 1999), SPUF (Brankart, 2013), SPP (Ollinaho, et al., 2017) and SKEB (Berner et al., 2009). The stochastic parameterizations in all schemes are implemented via first-order autoregressive Markov processes, i.e. a statistical model based on the assumption that the past value of uncertainty determines the present within some error. Several studies expand the NEMO ensemble framework (Bessières et al., 2017; Vervatis et al., 2021b), incorporating a stochastic ocean physics package (Storto and Andriopoulos, 2021).

The SPPT perturbs the net parameterized model tendencies, assumed to contain upscaled ocean model errors due to sub-grid parameterizations. The SPUF scheme is based on random walks sampling gradients (which represent the sub-grid unresolved scales) from the state vector and adding them to the models' solution; the random walks consist of independent consecutive steps in all directions. The SPP introduces perturbations at each time step to parameters within the model parameterization schemes. The SKEB adds perturbations to the barotropic stream function, upscaling a fraction of the dissipated energy back to the resolved flow, which is often useful assuming that the inverse cascade of energy is underestimated in ocean models due to unresolved sub-grid processes.

Selecting the appropriate perturbation scheme and properly tuning the stochastic parameterizations for the autoregressive processes (for each of the perturbed model quantities) are essential steps to produce meaningful stochastic ensembles. All stochastic perturbation schemes have their advantages and disadvantages (e.g. energy and mass conservation laws, production of over/under-dispersive ensembles, etc.), though the SPPT scheme appears to be the most effective (in terms of generating sufficient model spread) and easiest to use (in terms of stochastic parameterizations) for many model quantities.

A common approach to generate stochastic ocean model ensembles is by using a pseudorandom combination of multivariate empirical orthogonal functions (EOFs) to perturb the wind forcing (Vervatis et al., 2016). The wind has a large impact on upper-ocean model uncertainties because it controls the Ekman and geostrophic components of the Sverdrup dynamics; it

also largely drives the shelf-seas dynamics in addition to tides. In general, all surface atmospheric forcing variables constitute major sources of ocean model uncertainties. Momentum, heat, and freshwater fluxes are key quantities coupling the air-sea processes and are parametrized in terms of bulk coefficients. These model parameters can also be stochastically perturbed (in addition to atmospheric forcing) with spatiotemporal varying patterns (or by applying simple Gaussian noise, if there is no information available regarding their scales).

Complementary to stochastic approaches, ocean model uncertainties can be introduced by making use of an atmospheric ensemble. Using an atmospheric EPS does not necessarily outperform the stochastic modelling approach in terms of ocean model spread. In general, it takes longer for the ensemble to spin-up and increase its spread, and the method also requires a large amount of data to process. On the other hand, the main advantage of using an atmospheric EPS is the realism of the fields in terms of conserved quantities. A common approach of a marine EPS generated by an atmospheric EPS, used successfully at operational centres, is the ocean wind-wave ensemble forecasting (Janssen, 2004).

In the ocean interior below the seasonal thermocline, model uncertainties can be introduced effectively by perturbing the ocean boundary conditions and the water column properties. Such perturbations are usually difficult to implement because of the need to ensure physical consistency in the water column, and because errors in the prescribed boundary fields are usually unknown. A favourable solution for the open boundaries is when a coarse parent ensemble is available providing uncertainty estimates to the nested child model (Ghantous et al., 2020).

Methods incorporating polynomial chaos expansions along with EOF-based perturbations of temperature and salinity profiles in isopycnal coordinate space, can be applied efficiently in estimating model error propagation in the open boundaries (Thacker et al., 2012). Model uncertainties affecting also the water column properties can be applied in the equation of state by perturbing the temperature and salinity state, using the SPUF method aimed at representing sub-grid unresolved scales. Other quantities that can be perturbed in the ocean interior and its boundaries are the model bathymetry influencing the barotropic and baroclinic states (Lima et al., 2019), the bottom drag coefficient affecting the bottom Ekman flow transport and tidal mixing in shelf-seas (Vervatis et al., 2021b), and the SSH together with depth integrated velocities in tidal open boundaries (Barth et al., 2009).

Inflation methods and bred vectors for short-range ocean prediction systems can be used to initialise an ensemble of forecasts. The choice of perturbing initial conditions is also relevant to DA, for example using ensemble-based hybrid variational methods such as the 4D-EnsVar controlling (possibly among other quantities) the initial conditions.

Ensemble-based DA methods are used to improve the predictive skill of biogeochemical and sea-ice models. In these Earth system components, model errors stem from unresolved diversity, unresolved scales, and multiple model parameterizations. The unresolved diversity refers for example to the biodiversity restriction, including only a few species in the biogeochemical model, and to restrictions in the categorization of sea-ice in an effort to reduce complexity and state variables. These diversity restrictions often lead to missing model processes that are instead approximated by parameterizations. On the other hand, the unresolved scales depend on the model resolution (in a way similar to the unresolved scales for physics).

In this context, the most common quantities to perturb in biogeochemical models are the sources and sinks (e.g. photosynthesis, respiration, death, and grazing), and the biogeochemical parameters controlling some of these processes (e.g. growth and mortality rates, nutrient limitations, grazing, etc.) (Santana-Falcón et al., 2020). Other biogeochemical model state uncertainties depend on the water column optical properties and the penetrative solar radiation, affecting photosynthesis and primary production (Ciavatta et al., 2014). An anamorphosis transformation in lognormal space is required for any use of the stochastic biogeochemical outputs that involve Gaussian distributions, such as variance analysis or DA (Simon and Bertino, 2009). This latter attribute of selecting a positive distribution function to introduce model uncertainties is also followed for sea-ice perturbations, e.g. using a gamma distribution for the sea-ice strength variable to improve DA and model performance for sea-ice concentration and sea-ice thickness (Juricke et al., 2013).

5.6.3. Towards ocean EPS

A summary of the practical aspects and challenges of a roadmap towards ocean probabilistic forecasting for the next generation of OOFS is as follows. Initially, ensemble forecasting should be developed and tested without the use of DA. This will allow operational centres to coordinate their activities, such as: (a) preparing OGCM platforms for the production of ensembles, e.g. several choices among regional centres tuning the stochastic parameterizations; (b) integrating ensembles in their operational chain assessing the computational cost (doubled for DA) and which variables are essential to archive; and (c) providing tools for the interpretation of uncertainty estimates as well as guiding users to extract information from ensembles, e.g. ocean indices for the probabilistic detection of events. An open issue in this first step, without DA, is how ensembles are going to be initialised in an operational context. In a second step, within a DA framework, the initialization of the ensemble is part of the DA process.

5.7. Validation strategies

As explained in Section 4.5.2, four classes of metrics (Figure 4.30) were defined and adopted by GODAE OceanPredict and have been extensively used for the validation of OO model products since the first validation and intercomparisons exercises (Crosnier and Le Provost, 2007; Ryan et al., 2015). It is indeed necessary to use a complete range of statistics and comparisons in space and time to properly assess the consistency, representativeness, accuracy, performance, and robustness of ocean model outputs. One of the first steps at all stages of the validation procedure is usually to compare the surface temperature (analysed, and at various forecast length) with contemporaneous satellite observations, which is a good example of CLASS1 metrics (Figure 5.11). Sea surface temperature is a signature of ocean-atmosphere interactions and it is critical for many maritime applications, while being one of the major sources of uncertainty for ocean model analyses and forecasts. This type of comparison allows a day-to-day control of atmospheric forcing inconsistencies and large scale features of the systematic biases can also be monitored on the longer terms.

Another important step is to check the local behaviour of the model analyses and forecast for several time frequencies (tidal, non-tidal) using fixed buoys observations, for instance for sea surface height against tide gauges (CLASS2 metrics, Figure 5.12). This type of metrics is essential for the overall assessment of the representativeness of a physical model solution. Many statistical estimators can be used to compare models to observations within this CLASS1 and CLASS2 framework, but also spectral analysis, extreme events characterization, and mesoscale feature detection can be performed at this stage. This surface "satellite" approach (2-dimensional with time) and local approach (1-dimension with time) must be combined with the monitoring of the basin scale or global scale behaviour of the ocean, integrated in space (3-dimensions) and/or time, such as the validation and intercomparison

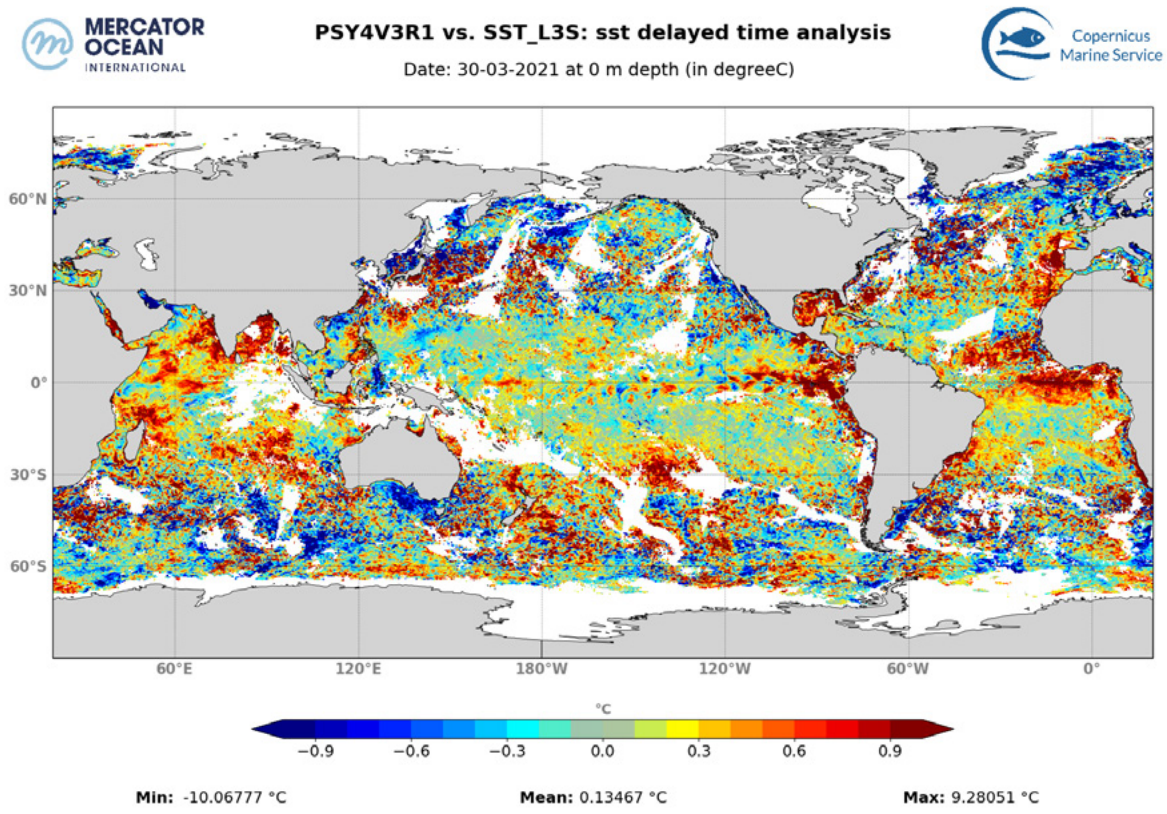

Figure 5.11. Copernicus Marine Service global model SST analysis minus gridded supercollated SST observations on 03/30/2021 (°C).

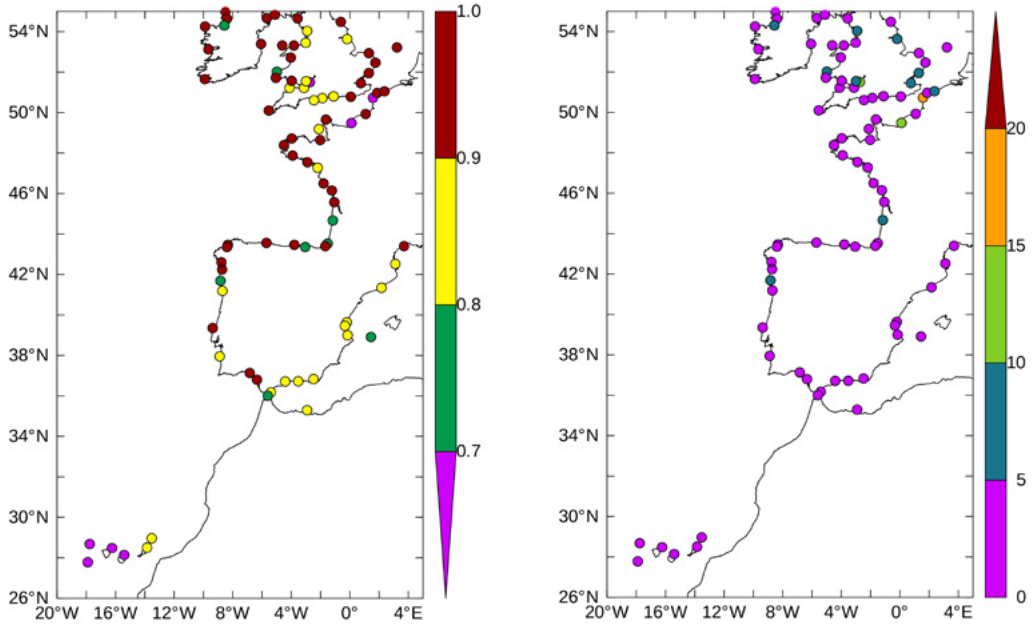

Figure 5.12. Correlation (left) and RMS difference (cm)(right) between the Iberia-Biscay-Ireland model analyses by Copernicus Marine Service and the observations of the residual elevation at tide gauges´ locations (January 2017 to December 2018) (courtesy of Bruno Levier, Mercator Océan).

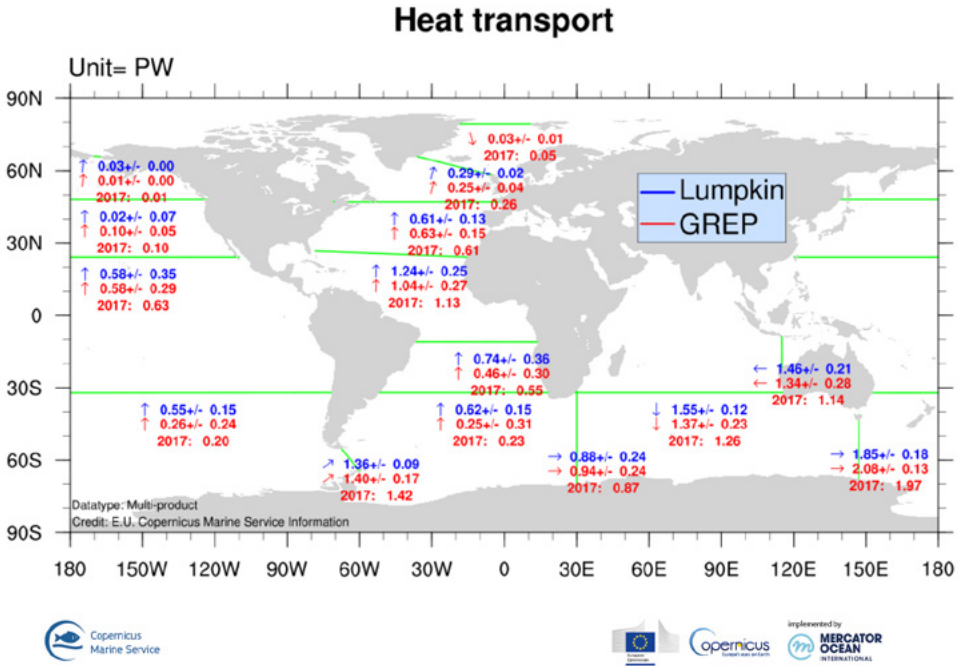

Figure 5.13. Heat transport (PW) from Copernicus Marine Service global reanalysis ensemble product ([8]) compared with estimates of Lumpkin and Speer (2007). Uncertainty ranges are derived from the ensemble standard deviation. Arrows indicate the direction of the mean flow through the sections.

8.https://marine.copernicus.eu/access-data/ocean-monitoring-indicators/mean-heat-transport-across-sections

of ocean monitoring indicators. The intercomparison of integrated heat transports (CLASS3 metrics, Figure 5.12) with values from the literature (Lumpkin and Speer, 2007) is a good example of diagnostic which can help identify biases, drifts or limitations in the model's representation of the ocean circulation, while it also provides valuable information on the ocean state and variability. Additionally, the intercomparison of several model estimates, whenever possible, allows to derive a range of likely values for ocean monitoring indicators, and to assess the robustness of the model solution. In Figure 5.13 the standard deviation between four ocean reanalyses (varying in their configuration and data assimilation

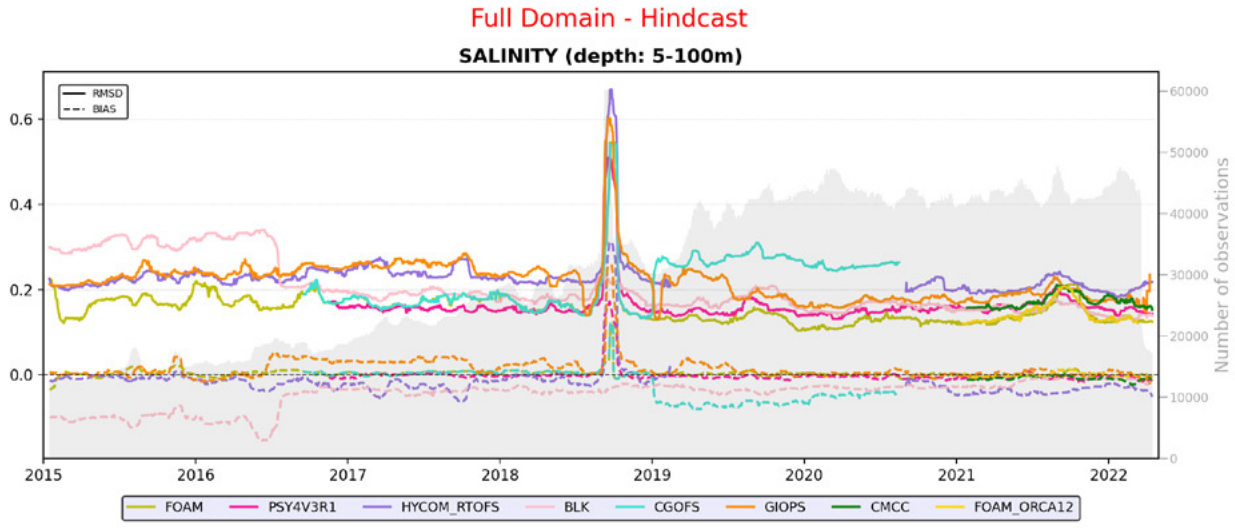

Figure 5.14. Performance of GODAE OceanPredict global forecasting systems, in terms of global mean departures from salinity in-situ profiles observations (psu) in the 0-500m layer. The time evolution of the mean bias between the model forecast (12h) and the observations is shown by dotted lines, and the root mean square difference is shown by solid lines (courtesy of Charly Régnier, Mercator Ocean).

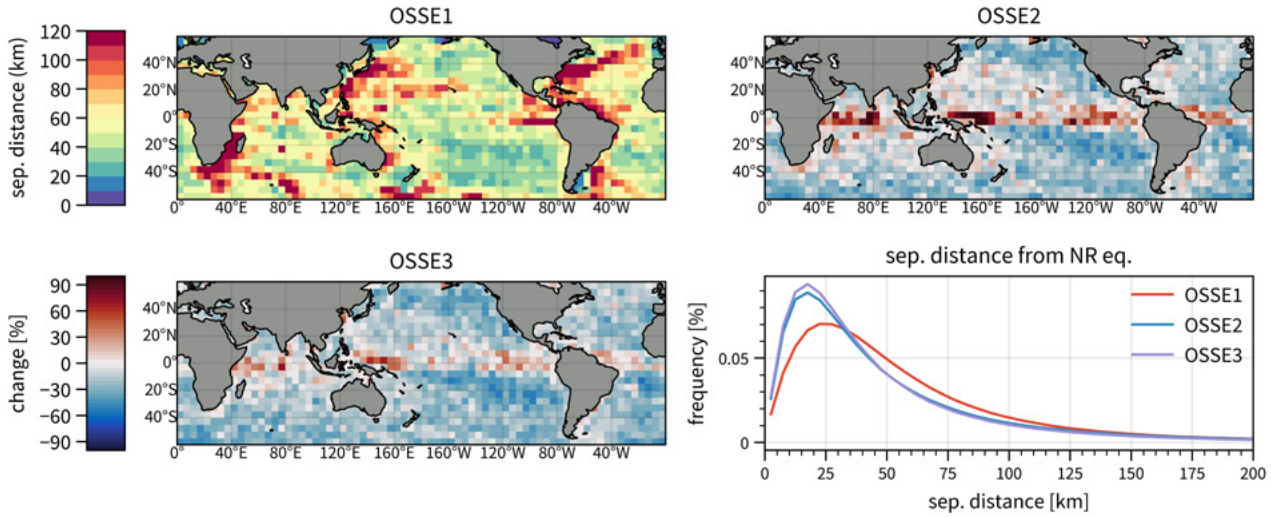

Figure 5.15. Results of a Lagrangian experiment. Panels: a) the metric corresponds to the distance separating the true position of the particle in NR with that of the OSSE1 (3Nadir) after 7 days, averaged in 5-degree bins; b) and c) show the average change in separation distance (reduction in blue) obtained when using instead OSSE2 and OSSE3 surface currents, with an overall improvement; and d) global distributions of the separation distance in each experiment (courtesy of Simon van Gennip, Mercator Ocean).

settings) based on the same model (NEMO) were used to derive the uncertainty associated with each heat transport estimate.

Finally, CLASS1-2-3 must be complemented by quality indicators averaged in space at basin scale, and possibly in time, in order to monitor and quantify the individual performance of model solutions. To this aim, data assimilation misfits (innovations and residuals) are extensively used, as observation operators, developed within data assimilation schemes, usually provide the most adequate transposition of the model solution into the observations' space. CLASS4 metrics can be computed offline in delayed time, outside of the data assimilation process, to add the possibility to compare residual differences with one given observation between various forecast lengths, to compare with climatology and persistence, and finally to derive forecast skill scores. Hence, independent observations (not assimilated) can be used to compute CLASS4 metrics, and reference datasets can be defined to build robust intercomparison frameworks. For instance, ARGO floats measurements are only used by the GODAE OceanPredict community in order to measure performance in salinity as illustrated by Figure 5.14 (Ryan et al., 2015). A spike in the statistics corresponds to a campaign at sea in the Arctic in 2018, which shows that, despite a growing observing network, these statistics suffer from representativeness issues.

As at high resolution (a few km or less) the small scales are not constrained by observations, the performance measured by direct or statistical comparisons to observations may not be as good as for coarser model solutions, which is referred to as the "double penalty" effect (Ebert, 2009). Neighbourhood metrics (Mittermaier et al., 2013, 2021) focus on the ability of a model to forecast a range of events within a neighbourhood in space and time, and for which the direct or statistical comparisons to observations at all time and space scales would not be informative.

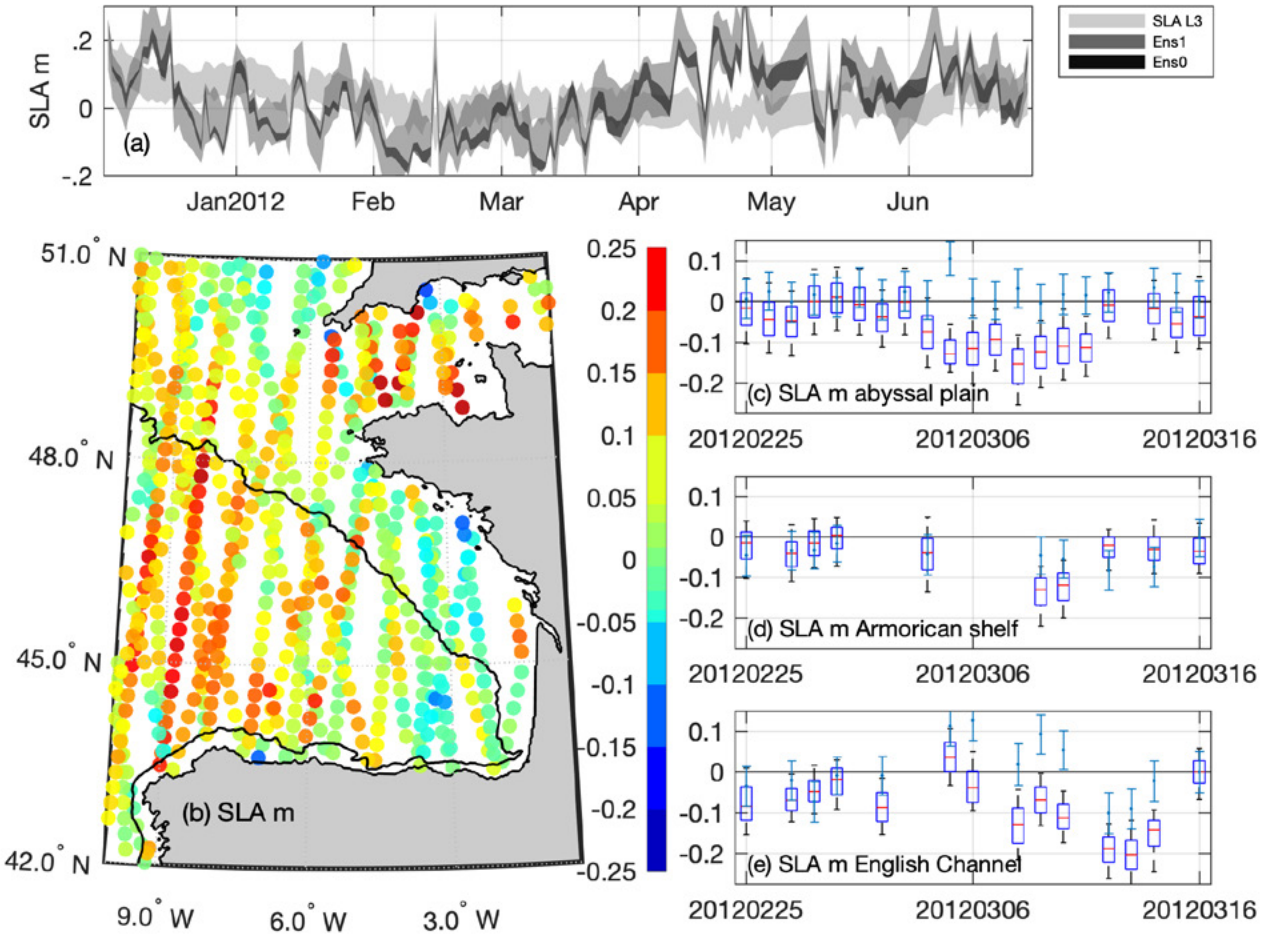

Figure 5.16. a) SLA along track L3 observation distribution (in meters) and two model ensembles in data space; (b) "Observation minus Ensemble" map for a period starting on 25 February 2012 and for three consecutive weeks; (c) box-whisker plots and observation error bars averaged over the abyssal plain; (d) the Armorican shelf; and (e) the English Channel.

Additionally, "user oriented" metrics focusing on processes or using downstream applications can reduce this effect and allow to better assess the fit-for-purpose of ocean analyses and forecasts, among which we can cite eddies (Mason et al., 2014), fronts detection (Ren et al., 2021), and lagrangian drift scores. Lagrangian separation distance scores and distributions (shown in Figure 5.15) are a primary validation diagnostic when studying the impact of changes in the observations network (Tchonang et al., 2021). Figure 5.15 shows, in particular, results of a Lagrangian experiment wherein particles seeded in every model grid cell (1/12 degree resolution) and advected for 7 days in the Nature Run and three different OSSEs surface currents (OSSE1 collecting and assimilating 3 nadir-like satellite altimeters, and OSSE2 SWOT-like satellite altimeter, and OSSE3 nadir-like and one SWOT-like satellite altimeters).

Ensemble scores applied to ensemble forecasts (see Section 5.6) also allow better study of predictability and, eventually, to validate and quantify the skill of the forecast. This is needed in particular for mesoscale features (Thoppil et al,. 2021). In the near future, it is essential to add this type of verification and quantification of uncertainty to the range of validation metrics. Figure 5.16 illustrates examples of ensemble diagnostics (Vervatis et al., 2021a) important to be checked in the development phase and during the production to verify consistency between ensemble model distribution and observation. Figure 5.16a compares the distribution of observations (light grey) and of two ensemble simulations (dark grey); a good quality criterion is the distribution of ensemble members overlapping the distribution of the observations, if this should not be investigated. Figure 5.16b shows the bias between ensemble members and observations in the observations' space for a dedicated period. Errors can also be quantified in physically consistent domains as illustrated in Figure 5.16c, where the consistency between box-whisker plots of the ensemble members distributions and error bars can be assessed for observations in the same area.

5.8. Outputs

Information on formats and types of outputs of all kinds of OOFS can be found in Chapter 4. The following section treats only some specific aspects related to circulation modelling.

5.8.1. Variables/EOV

The circulation modelling variables describe any system related to the production of 3D ocean dynamics variables.

The main physics variables (with their abbreviation or acronym) are:

- Temperature
  - temperature [T]
  - sea surface temperature [SST]
  - bottom temperature bottom [bottomT]
- Density [D]
- Salinity [S]
- Sea Surface Height [SSH]
  - above sea level
  - above geoid
  - geopotential height
- Velocity
- Velocity [UV/W]
  - geostrophic velocity [UV/UVG]
  - barotropic velocity [UVB]
- Mixed Layer Depth [MLD]
- Sea Ice
  - sea ice concentration [SIC]
  - sea ice edge [SIE]
  - sea ice extent [SIE]
  - sea ice thickness [SIT]
  - sea ice velocity [SIUV]
  - sea ice drift [SIUV]
  - snow [SNOW]
  - iceberg [ICBG]
  - sea ice age [SIAGE]
  - sea ice albedo [SIALB]
  - sea ice temperature [IST]

The variables follow the CF standards. The CF Metadata Conventions are a widely used standard for atmospheric, ocean, and climate data. Standard names are defined in a CF Standard Name Table (see [9]).

9. http://cfconventions.org/standard-names.html

5.9. Inventories

The purpose of this section is to provide an initial inventory of the operational Near Real Time (NRT) and Multi Year (MY) systems operating at international level. Details about the specific system, resolution, implemented circulation model, and data assimilation are provided in the following lists, along with the observations used for assimilation and assessment, summary of the main offered product catalogue and, where existing, the website address to directly link to systems products and other relevant information.

5.9.1. Inventory of operational global to regional to coastal to local forecasting systems

The present state-of-the-art operational systems for NRT products from global to local scale is presented in Table 5.2. This proposed inventory has been prepared in collaboration with the Coastal and Shelf Seas (COSS-TT) Working Group, one of the OceanPredict Task Teams. An evolutive list of Regional/Coastal Ocean Forecasting Systems (R/COFS) is maintained by the COSS-TT in the System Information Table (SIT) (latest version available at [10]). Due to the shorter lifespan and more frequent updates in coastal systems compared to global and basin-scale systems, the SIT is frequently refreshed and then please refer to the latest online version for up-to-date information. In addition to operational/NRT systems, the online SIT contains also tools (e.g. used for applications, crisis-time scenarios, etc.), research and pre-operational models, etc.

5.9.2. Inventory of multi-year systems

Starting from the list in Balmaseda et al. 2015, an initial inventory of state-of-the-art MY systems has been prepared (Table 5.3). As in Table 5.2, for each system is provided scale (from global to regional), resolution, models, and providers, as well as relevant links to web pages that the reader may consult for further details.

10. https://oceanpredict.org/science/task-team-activities/coastal-ocean-and-shelf-seas/#section-sit

Table 5.2. Initial inventory of global (G) to regional (R) to coastal (C) to local (L) operational forecasting systems.

Scale	System	Area	Resolution	Circulation model	Data used for assimilation and assessment	Downscaling/ nesting	Products	Website
G	OceanMAPS, BLUElink (Bureau of Meteorology)	Global ocean	0.1 degree grid spacing at the Australia region	MOM4	BODAS is an ensemble optimal interpolation system used to assimilate available in-situ and satellite obs.	N/A	Daily T, S, SSH and UV	https://research.csiro.au/bluelink/global/forecast/
G	CONCEPTS GIOPS (Government of Canada)	Global ocean	1/4° horizontal resolution	NEMO	SEEK scheme, using INS, SLA, SST obs.	N/A	Daily 10-days forecast for T, S, SSH, UV, sea ice concentration	https://science.gc.ca/eic/site/063.nsf/eng/h_97631.html
G	ECCO: Estimating the Circulation and Climate of the Ocean	Global ocean	The horizontal resolution varies spatially from 22 km to 110 km	MITgcm	Assimilation of INS, SLA, SST obs.	N/A	Daily forecast for T, S, SSH, UV, fluxes, sea ice	https://ecco-group.org/products-ECCO-V4r4.htm
G	FOAM: Forecast Ocean Assimilation Model system	Global ocean	1/4° horizontal resolution	NEMO	NEMOVAR (3D-Var scheme) using INS, SLA, SST obs.	N/A	Daily mean, analysis and five-day forecast for T, S, SSH, UV, sea ice	https://www.metoffice.gov.uk/research/weather/ocean-forecasting
G	NAVOCEANO, the US Naval Oceanographic Office (US)	Global ocean	1/12° horizontal resolution	HYCOM	Hybrid data assimilation scheme	N/A	Daily forecast for ocean fields	https://www.metoffice.gov.uk/research/weather/ocean-forecasting
G	INCOIS, the Indian National Centre for Ocean Information Service	Global ocean	horizontal resolution at 1/4° with 40 vertical sigma levels	ROMS	N/A	N/A	Daily 5 days forecast for surface UV, SST, MLD, waves and winds	https://incois.gov.in/

Scale	System	Area	Resolution	Circulation model	Data used for assimilation and assessment	Downscaling/ nesting	Products	Website
G	GOFS16 CMCC Global Ocean Forecasting System	Global ocean	1/16° horizontal resolution and 98 vertical levels	NEMO	OceanVar (3D-Var scheme) using INS, SL, SST, SICE obs.	N/A	Daily analysis and 7 days forecast for T, S, SSH, UV, sea ice	https://gofs.cmcc.it/
G	Global MFC by Copernicus Marine Service (MOI, France)	Global ocean	1/12° horizontal resolution and 50 vertical levels	NEMO	SAM2 (SEEK scheme) using INS, SLA, SST obs.	N/A	Daily analysis and 10 days forecast for T, S, SSH, UV, sea ice	https://marine.copernicus.eu
G/R	MOVE/MRI.COM-JPN (MRI, Japan)	Global, North Pacific, Japan	Double nested system consisting of global (GLB), North Pacific (NP) and Japan area (JPN) models Ocean model : MRI.COM with resolutions: (JPN) 1/33° x 1/50°, 60 levels; (NP) 1/11° x 1/10°, 60 levels; (GLB) 1°x1/2° (tripolar), 60 levels	MRI.COM	4DVAR (applied to a reduced grid version of NP model). Assessment: Tide gauge, In-situ observations (buoy, T-S profiles), HF radars, satellite (SST, SSH, sea ice concentration), volume transport at repeated hydrographic sections.	Downscaling: one/two-way nesting with IAU initialization	Real time monitoring and prediction, reanalysis of: T, S, UV, SSH, sea ice concentration, tropical cyclone heat potential (TCHP)	https://ds.data.jma.go.jp/tcc/tcc/products/elnino/move_mricom-g2_doc.html
R	Arctic MFC by Copernicus Marine Service (NERSC, Norway)	Arctic Region	12.5 km at the North Pole	HYCOM	EnKF assimilation scheme using INS, SLA, SST and SICE obs.	N/A	Daily analysis and 10 days forecast for T, S, SSH, UV, sea ice	https://marine.copernicus.eu
R	Baltic MFC by Copernicus Marine Service (SHMI, Sweden)	Baltic Sea	0.028 degrees x 0.017 degrees in horizontal and 56 levels	NEMO	PDAF LESTKF univariate for SST	1-way nested into NWS-MFC Copernicus Marine Service regional product	Daily analysis and 6 days forecast for T, S, SSH, MLD, UV	https://marine.copernicus.eu
R	Mediterranean Sea MFC by Copernicus Marine Service (CMCC, Italy)	Mediterranean Sea	1/24° in horizontal and 141 vertical levels, 2-way coupled to WW3 wave model	NEMO	OceanVar (3D-Var scheme) using INS, SL, SST obs.	1-way nested into GLO-MFC Copernicus Marine Service (1/12°, 50 vertical levels)	Analysis and 10 days forecast for T, S, SSH, UV, MLD, fluxes, sea icea	https://marine.copernicus.eu, https://medfs.cmcc.it/

Scale	System	Area	Resolution	Circulation model	Data used for assimilation and assessment	Downscaling/ nesting	Products	Website
R	Irish-Biscay-Iberian shelves MFC by Copernicus Marine Service (Mercator Ocean International, France / Spain)	Irish-Biscay-Iberian shelves	1/36° in horizontal and 50 vertical levels	NEMO	SEEK scheme, using INS, SL, SST obs.	1-way nested into GLO-MFC Copernicus Marine Service (1/12°, 50 vertical levels)	Analysis and 5 days forecast for T, S, SSH, UV, MLD	https://marine.copernicus.eu
R	North-West shelf MFC by Copernicus Marine Service (Met Office, UK)	European North-West shelf Seas	1.5 km in horizontal and 51 hybrid s-sigma terrain-following coordinates on the vertical	NEMO	NEMOVAR (3D-Var scheme) using INS, SL, SST obs.	1-way nested into Met Office FOAM NATL (1/12°; 6 hourly fields) and Baltic Sea physics by Copernicus Marine Service (2 km, 1 hourly fields)	Analysis and 5 days forecast for T, S, SSH, UV, MLD	https://marine.copernicus.eu
R	Black Sea MFC by Copernicus Marine Service (CMCC, Italy)	Black Sea	1/40° in horizontal and 121 vertical levels	NEMO	OceanVar (3D-Var scheme) using INS, SL, SST obs.	Lateral open boundary conditions from the Unstructured Turkish Straits System (U-TSS, Ilicak et al. 2021)	Analysis and 10 days forecast for T, S, SSH, UV, MLD	https://marine.copernicus.eu
R	High Resolution Data Assimilative Model for Coastal and Shelf Seas around China (Institute of Atmospheric Physics/Chinese Academy of Sciences, China)	Northwest Pacific, coastal seas around China			Assessment: SST, SLA, temperature, buoys, ship cruises	2-way nesting	Daily averaged 3-D fields of UV, T, S	

Scale	System	Area	Resolution	Circulation model	Data used for assimilation and assessment	Downscaling/ nesting	Products	Website
R/C	MARC: Modelling and Analyses for Coastal Research and ILICO: Coastal Ocean and Nearshore Observation Research Infrastructure (Ifremer, France)	Bay of Biscay / English Channel / Northwestern Mediterranean Sea	2.5 km horizontal resolution and 40 levels	MARS3D	SST, HF Radar (sea state + currents), Moored buoys (T,S)	Spectral nudging, one-way nesting using GLO-MFC products and 2D models for tides	1 hr output in Bay of Biscay, 3 hr output in Mediterranean Sea, HF observations (20min)	MARC: http://marc.ifremer.fr ILICO: https://www.ir-ilico.fr/en
R/C	SOMISANA (SAEON/DFFE, South Africa)	Algoa Bay, south coast, South Africa	Horizontal grid that decreases from ~3km at the edges to 500 m within the bay	CROCO	No DA. Assessment is based on Underwater Temperature Recorder (UTR) and ADCP data	1-way nested into GLO-PHY (1/12°, 50 vertical levels)	SSH, 3D T, S and UV, trajectories from hypothetical oil spills	http://ocim-stest.ocean.gov.za/aloga_bay_model
R/C	CNAPS Coupled Northwest Atlantic Prediction System (North Carolina State University, USA)	Northwest Atlantic coast ocean, including the entire east coast of U.S., the Gulf of Mexico and Caribbean seas	Horizontal resolution < 7 km	ROMS	HF Radar, buoy, ship, satellite observations	1-way nesting with Mercator Ocean GLO-PHY; Global HyCOM; WWIII	Daily nowcast and 3-day forecast for UV, T, S, ocean waves and atmospheric variables	http://omgsrv1.meas.ncsu.edu:8080/CNAPS/
R/C	REMO Oceanographic Modeling and Observation Network (Brazilian Navy Hydrographic Center, Brazil)	Region between latitudes 35.5°S and 7°N and longitude 20°W to the Brazilian coast	2 grids, at 1/12° and 1/24° horizontal resolutions for the eastern, southeastern and southern regions	HYCOM	The system assimilates vertical profiles of temperature (T) and salinity (S) from the ARGO system, XBTs, CTDs, Sea Level Anomaly, SST; assessment using AVISO SL, SST, INS	TPXO 7.1 for tides; one-way nesting from the 1/12° resolution to the 1/24° resolution grid	4-day forecasts (T, UV and SSH) at 6-hour intervals updated daily on 2 different grids	https://www.marinha.mil.br/chm/dados-do-smm-modelagem-numerica-tela-de-chamada/modelagem-numerica

Scale	System	Area	Resolution	Circulation model	Data used for assimilation and assessment	Downscaling/ nesting	Products	Website
R/C	DREAMS: Data assimilation Research of the East Asian Marine System (RIAM, Kyushu University, Japan)	Northwestern Pacific with focus on marginal seas	DREAMS_marginal seas model at ~7.4km horizontal resolution. Coastal models at ~1.5km along the Japan Sea coast nested in DREAMS_ marginal seas model	RIAM	Assessment: Volume transport through the Tsushima Strait, U, V and T measurements by fishing vessels	OBC from climatological run	T, S, U, V, sea level, mixed layer depth, density	https://dreams-c1.riam.kyushu-u.ac.jp/vwp
R to L	BSH Operational Model System (BSH, Germany)	North and Baltic Sea, German coastal waters	Horizontal resolution is 3 km for the North and Baltic Sea, 0.5 km for German coastal waters	HBM	Assimilation with PDAF scheme using AVHRR SST/ Sentinel-3 SST and validation using Copernicus Marine Service data	2-way nesting among regional and coastal models	120-hour forecast from 0 and 12 UTC and a 78-hour forecast from 6 and 18 UTC; water level, T, S, UV, ice products and biogeochemical variables	https://www.bsh.de/EN/DATA/Predictions/predictions_node.html
R to L	COSYNA	North Sea, German Bight, German Wadden Sea	3 nested models: i) North Sea Baltic Sea model (5 km), ii) German Bight model (1 km, varying unstructured-grid, 1km), iii) Estuarine model (varying unstructured-grid, 20-200 m)	GETM	Assessment with independent ADCP observations, FerryBox data, dedicated profile measurements, intercomparison with products from other operational systems	MyOcean ECOOP, OSTIA, MERIS color data Downscaling using 3 different grids	Surface UV, T, S, suspended matter, wind wave characteristics in the German Bight	http://codm.hzg.de/codm

Scale	System	Area	Resolution	Circulation model	Data used for assimilation and assessment	Downscaling/ nesting	Products	Website
C	PCOMS: Portuguese Coastal Operational Modelling System (MARETEC, Portugal)	Western Iberia region and subregions	5.6 km in horizontal and 50 vertical layers	MOHID 3D	N/A	1-way nesting into Mercator-Ocean PSY2V4 in the North Atlantic; tidal levels computed by a 2D version of MOHID, forced by FES2004, running on a wider region. Climatological profiles from WOA09 for nutrients.	Hindcasts and 3-day forecasts of SSH and 3D UV, T, S and biogeochemical model	http://forecast.maretec.org
C	SANIFS (CMCC, Italy)	Southern Adriatic Northern Ionian coastal Forecasting System	Horizontal resolution from 3 km in open-sea to 100-20 m in coastal areas	SHYFEM	No DA. Assessment using available observations from Copernicus Marine Service, EMODnet and national observing network	1-way nesting using the Copernicus Marine Service Mediterranean MFC regional forecast products (at 1/24°)	Short term forecast (3 days) of SSH, 3D UV, T, S	http://sanifs.cmcc.it
C/L	SAMOA (Puertos del Estado, Spain)	Regional areas at ~ 2 km resolution; model applications consist of 2 nested regular grids with spatial resolution of ~350 m and ~70 m for the coastal and harbour domains	Regional areas at ~ 2 km resolution; model applications consist of 2 nested regular grids with spatial resolution of ~350 m and ~70 m for the coastal and harbour domains	ROMS	No DA. Assessment using in-situ obs. from mooring buoys, ADCPs, tide gauges and drifter buoys; SST satellite data and surface currents from HF radar	1-way nesting using the IBI-MFC Regional Forecast products (at 1/36°)	Daily operational short-term (+72h) met-ocean forecast	http://opendap.puertos.es/thredds/catalog.html ; http://www.puertos.es/es-es/proyectos/Paginas/SAMOA.aspx

Scale	System	Area	Resolution	Circulation model	Data used for assimilation and assessment	Downscaling/ nesting	Products	Website
C/L	NYHOPS: New York Harbor Observation and Prediction System (Jupiter Intelligence, USA)	New York and East Coast of US	7.5 km at the open ocean boundary to less than 50 m	POM	N/A	Offshore boundary tides, surges, waves. Real time data from Ntl Ocean Service, Adv. Hydrologic Prediction Service, Ntl. Climatic Data Center.	72 hr forecasts, nowcasts, 24 hr hindcasts initiated every 6 hrs; Variables: SSH, T, S, UV, winds, coastal waves - height, period and direction, biogeochemical variables	https://hudson.dl.stevens-tech.edu/maritimeforecast/index.shtml
C/L	SWITCH – Georgia Coasts (CMCC / GeorgiaTech, Italy / USA)	Georgia coast, US	1km in open ocean to 100m in coastal areas to 10m in the rivers	SHYFEM	No DA, assessment is based on tide gauges at coast and along rivers	1-way nested into GLO-PHY (1/12°, 50 vertical levels)	3-days forecast for SSH, 3D UV, T, S	https://savannah.cmcc.it
L	Tagus Mouth operational model (MARETEC / IST, Portugal)	Tagus Estuary and Mouth region	Variable horizontal resolution, ranging from 2 km off the coast up to 400 m inside the estuary, 50 layers in the vertical	MOHID 3D	No DA. Assessment: Argo and buoys data from IBI-ROOS and the Portuguese hydrographic institute, satellite images (ODYSSEA, Ocean Colour and HF radar)	1-way nesting using the PCOMS	Hindcasts and 3-day forecasts of SSH and 3D UV, T, S and biogeochemical model	http://forecast.maretec.org/tagusmouth

Table 5.3. Initial inventory of global (G) to regional (R) to coastal (C) to local (L) multi-year systems.

Scale	System	Area	Resolution	Circulation model	Data Assimilation scheme	Downscaling/ nesting	Timeseries	Website
G	CFSR by the Climate Prediction Center	Global Ocean	~ 38 km horizontal resolution and 64 vertical levels	MOM4	3D-Var scheme for the assimilation of SST, INS, SICE obs.	N/A	1979-2010	https://rda.ucar.edu/#!lfd?nb=y&b=proj&v=NCEP%20Climate%20Forecast%20System%20Reanalysis
G	C-GLORS by the Euro-Mediterranean Center on Climate Change Foundation	Global Ocean	1/4° horizontal resolution and 50 to 75 levels	NEMO	OceanVar (3D-Var scheme) using INS, SLA, SST and SICE obs.	N/A	1990-2016	http://c-glors.cmcc.it/index/index.html
G	ECCO by JPL-NASA	Global Ocean	The horizontal resolution varies spatially from 22 km to 110 km	MitGCM	4D-Var scheme for the assimilation of SLA, SST and INS obs.	N/A	1992-2017	www.ecco-group.org
G	GECCO by University of Hamburg	Global Ocean		MitGCM	4D-Var scheme for the assimilation of SLA, SST and INS obs.	N/A	1948-2018	www.ecco-group.org
G	ECDA by the Geophysical Fluid Dynamics Laboratory	Global Ocean	1° horizontal resolution and 50 vertical levels	MOM4	EnKF scheme using INS, SST and SLA obs.	N/A	Integration for the 20th Century	http://www.gfdl.noaa.gov/ocean-data-assimilation
G	GloSea5 (UK MetOffice, UK)	Global Ocean	1/4° horizontal resolution and 75 levels	NEMO	3D-Var scheme using SLA, SST, INS and SICE obs.	N/A	1993-2015	https://www.metoffice.gov.uk/research/

Scale	System	Area	Resolution	Circulation model	Data Assimilation scheme	Downscaling/ nesting	Timeseries	Website
G	K7-ODA (Japan Agency for Marine-Earth Science and Technology)	Global Ocean	1° horizontal resolution and 45 levels	MOM3	4D-Var adjont method for the assimilation of INS, SLA, SST obs.	N/A	1957-2009	http://www.godac.jamstec.go.jp/estoc/e/
G	PEODAS (Centre for Australian Weather and Climate Research - Bureau of Meteorology)	Global Ocean	1° x 2° horizontal resolution	MOM2	EnKF for the assimilation of INS and SST obs.	N/A	2000-2010	https://www.cawcr.gov.au/
G	ORAS5 (ECMWF, UK)	Global Ocean	1° horizontal resolution	NEMO	3D-Var scheme using SLA, INS and SST obs.	N/A	1979-present	https://www.ecmwf.int/en/research/climate-reanalysis/ocean-reanalysis
G	MOVE-C RA (Japan Meteorological Agency)	Global Ocean	1° horizontal resolution	MRI.COM2	3D-Var scheme using SLA, INS and SST obs.	N/A	1950-2011	https://www.mri-jma.go.jp/
G	SODA (National Center for Atmospheric Research Staff, US)	Global Ocean	1/4° horizontal resolution	POP2.1	OI for INS and SST obs.	N/A	1869-2010	https://climatedataguide.ucar.edu/climate-data/soda-simple-ocean-data-assimilation
G	Global Ocean MFC by Copernicus Marine Service (MOI, France)	Global Ocean	1/12° horizontal resolution, 50 vertical levels	NEMO	Reduced-order Kalman filter for assimilating SLA, SST, INS and SICE obs.	N/A	1993-2019	https://marine.copernicus.eu
R	Arctic MFC by Copernicus Marine Service (NERSC, Norway)	Arctic Region	12.5 km horizontal resolution and 12 levels	HYCOM	DEnKF for assimilating satellite and INS obs.	N/A	1991-2019	https://marine.copernicus.eu

Scale	System	Area	Resolution	Circulation model	Data Assimilation scheme	Downscaling/ nesting	Timeseries	Website
R	Baltic MFC by Copernicus Marine Service (SHMI, Sweden)	Baltic Sea	0.05556 degrees x 0.03333 degrees horizontal resolution and 56 vertical levels	NEMO	LSEIK data assimilation scheme	At the lateral boundaries in the western English Channel and along the Scotland-Norway boundary, the sea levels are prescribed using a coarse (24 nautical miles resolution) storm-surge model called NOAMOD (North Atlantic Model). Climatological monthly mean values of salinity and temperature are used at the boundary, and it is assumed there is no sea ice	1993-2019	https://marine.copernicus.eu
R	North-West shelf MFC by Copernicus Marine Service (Met Office, UK)	North West Shelf Seas	7 km horizontal resolution and 24 vertical levels	NEMO	NEMOVAR (3D-Var scheme) using SST and INS obs.	1-way nested into the Global Ocean MFC and Baltic MFC reanalysis products	1993-2019	https://marine.copernicus.eu
R	Irish-Biscay-Iberian shelves MFC by Copernicus Marine Service (Puertos del Estado, Spain)	Irish-Biscay-Iberian shelves	1/12° horizontal resolution	NEMO	SEEK scheme, using INS, SL, SST obs.	1-way nested into the Global Ocean MFC reanalysis product at 1/4° horizontal resolution	1993-2019	https://marine.copernicus.eu
R	Mediterranean Sea MFC by Copernicus Marine Service (CMCC, Italy)	Mediterranean Sea	1/24° in horizontal and 141 vertical levels	NEMO	OceanVar (3D-Var scheme) using INS, SLA, SST obs.	1-way nested into C-GLORS	1993-2019	https://marine.copernicus.eu
R	Black Sea MFC by Copernicus Marine Service (CMCC, Italy)	Black Sea	3 km horizontal resolution and 31 vertical levels	NEMO	OceanVar (3D-Var scheme) using INS, SLA, SST obs.	N/A	1993-2019	https://marine.copernicus.eu

5.10. References

Balmaseda, M. A., Mogensen, K., and Weaver, A.T. (2013). Evaluation of the ECMWF ocean reanalysis system ORAS4. Quarterly Journal of the Royal Meteorological Society, 139, 1132-1161, https://doi.org/10.1002/qj.2063

Balmaseda, M.A., Hernandez, F., Storto , A., Palmer, M.D., Alves, O., Shi, L., Smith, G.C. Toyoda, T., Valdivieso, M., Barnier, B., Behringer, D., Boyer, T., Chang, Y-S., Chepurin, G.A., Ferry, N., Forget, G., Fujii, Y., Good, S., Guinehut, S., Haines, K., Ishikawa, Y., Keeley, S., Köhl, A., Lee, T., Martin, M.J, Masina, S., Masuda, S., Meyssignac, B., Mogensen, K., Parent, L., Peterson, K.A., Tang, Y.M., Yin, Y., Vernieres, G., Wang, X., Waters, J., Wedd, R., Wang, O., Xue, Y., Chevallier, M., Lemieux, J.F., Dupont, F., Kuragano, T., Kamachi, M., Awaji, T., Caltabiano, A., Wilmer-Becker, K., Gaillard, F. (2015). The Ocean Reanalyses Intercomparison Project (ORA-IP). Journal of Operational Oceanography, 8(sup1), s80-s97, https://doi.org/10.1080/1755876X.2015.1022329

Barth, A., Alvera-Azcárate, A., Beckers, J.M., Weisberg, R. H., Vandenbulcke, L., Lenartz, F., and Rixen, M. (2009). Dynamically constrained ensemble perturbations–application to tides on the West Florida Shelf. Ocean Science, 5, 259-270, https://doi.org/10.5194/os-5-259-2009

Bell, M., Schiller, A., Le Traon, P-Y., Smith, N.R., Dombrowsky, E., Wilmer-Becker, K. (2015). An introduction to GODAE OceanView. Journal of Operational Oceanography, 8, 2-11, https://doi.org/10.1080/1755876X.2015.1022041

Bennett, A.F. (1992). Inverse Methods in Physical Oceanography, Cambridge University Press, Cambridge, UK.

Berner, J., G. Shutts, M. Leutbecher, and T. Palmer. (2009). A spectral stochastic kinetic energy backscatter scheme and its impact on flow-dependent predictability in the ECMWF ensemble prediction system. Journal of the Atmospheric Sciences, 66, 603-626, https://doi.org/10.1175/2008JAS2677.1

Bessières, L., Leroux, S., Brankart, J.M., Molines, J.M., Moine, M.P., Bouttier, P.A., Penduff, T., Terray, L., Barnier, B., Sérazin, G. (2017). Development of a probabilistic ocean modelling system based on NEMO 3.5: Application at eddying resolution. Geoscientific Model Development, 10, 1091-1106, https://doi.org/10.5194/gmd-10-1091-2017

Bjerknes, V. (1914). Meteorology as an exact science. Monthly Weather Review, 42(1), 11-14, https://doi.org/10.1175/1520-0493(1914)42<11:MAAES>2.0.CO;2

Blayo, E., and Debreu, L. (1999). Adaptive mesh refinement for finite-difference ocean models: first experiments. Journal of Physical Oceanography, 29(6), 1239-1250, https://doi.org/10.1175/1520-0485(1999)029<1239:AMRFFD>2.0.CO;2

Blayo, E., and Debreu, L. (2005). Revisiting open boundary conditions from the point of view of characteristic variables. Ocean Modelling, 9(3), 231-252, https://doi.org/10.1016/j.ocemod.2004.07.001

Bouttier, F., and Courtier, P. (2002). Data assimilation concepts and methods, March 1999. ECMWF Education material, 59 pp., https://www.ecmwf.int/en/elibrary/16928-data-assimilation-concepts-and-methods

Brankart, J.-M., (2013). Impact of uncertainties in the horizontal density gradient upon low resolution global ocean modelling. Ocean Modelling, 66, 64-76, http://dx.doi.org/10.1016/j.ocemod.2013.02.004

Brankart, J.-M., Candille, G., Garnier, F., Calone, C., Melet, A., Bouttier, P.-A., Brasseur, P., Verron, J., (2015). A generic approach to explicit simulation of uncertainty in the NEMO ocean model. Geoscientific Model Development, 8, 1285-1297, https://doi.org/10.5194/gmd-8-1285-2015

Brassington, G.B., Warren, G., Smith, N., Schiller, A., Oke, P.R. (2005). BLUElink> Progress on operational ocean prediction for Australia. Bulletin of the Australian Meteorological and Oceanographic Society, Vol.18 p. 104.

Buizza, R., Miller, M., Palmer, T.N. (1999). Stochastic representation of model uncertainties in the ECMWF ensemble prediction system. Quarterly Journal of the Royal Meteorological Society, 125, 2887-2908, http://dx.doi.org/10.1002/qj.49712556006

Candille, G., and Talagrand, O. (2005). Evaluation of probabilistic prediction systems for a scalar variable. Quarterly Journal of the Royal Meteorological Society, 131, 2131-2150, https://doi.org/10.1256/qj.04.71

Charria, G., Lamouroux, J., De Mey, P. (2016). Optimizing observational networks combining gliders, moored buoys and FerryBox in the Bay of Biscay and English Channel. J. Mar. Syst., 162, 112-125. http://dx.doi.org/10.1016/j.jmarsys.2016.04.003

Chassignet, E. P., Hurlburt, H. E., Smedstad, O. M., Halliwell, G. R., Hogan, P. J., Wallcraft, A. J., and Bleck, R. (2006). Ocean prediction with the hybrid coordinate ocean model (HYCOM). In "Ocean weather forecasting", 413-426, Springer, Dordrecht, doi:10.1007/1-4020-4028-8_16

Chelton, D. B., DeSzoeke, R. A., Schlax, M. G., El Naggar, K., and Siwertz, N. (1998). Geographical variability of the first baroclinic Rossby radius of deformation. Journal of Physical Oceanography, 28(3), 433-460, https://doi.org/10.1175/1520-0485(1998)028<0433:GVOTFB>2.0.CO;2

Cheng, S., Aydoğdu, A., Rampal, P., Carrassi, A., Bertino, L. (2020). Probabilistic Forecasts of Sea Ice Trajectories in the Arctic: Impact of Uncertainties in Surface Wind and Ice Cohesion. Oceans, 1, 326-342, https://doi.org/10.3390/oceans1040022

Ciavatta, S., Torres, R., Martinez-Vicente, V., Smyth, T., Dall'Olmo, G., Polimene, L., and Allen, J. I. (2014). Assimilation of remotely-sensed optical properties to improve marine biogeochemistry modelling. Progresses in Oceanography, 127, 74-95, https://doi.org/10.1016/j.pocean.2014.06.002

Crosnier, L., and Le Provost, C. (2007). Inter-comparing five forecast operational systems in the North Atlantic and Mediterranean basins: The MERSEA-strand1 Methodology. Journal of Marine Systems, 65(1-4), 354-375, https://doi.org/10.1016/j.jmarsys.2005.01.003

Cummings, J. A. (2005). Operational multivariate ocean data assimilation. Quarterly Journal of the Royal Meteorological Society, 131(613), 3583-3604, https://doi.org/10.1256/qj.05.105

Cummings, J.A., and Smedstad, O.M. (2013). Variational data analysis for the global ocean. In: S.K. Park and L. Xu (Eds.), Data Assimilation for Atmospheric, Oceanic and Hydrologic Applications Vol. II., doi:10.1007/978-3-642-35088-7_13, Springer-Verlag Berlin Heidelberg.

Daley, R. (1991). Atmospheric Data Analysis. Cambridge University Press. 457 pp.

Danilov, S., Kivman, G., and Schröter, J. (2004). A finite-element ocean model: principles and evaluation. Ocean Modelling, 6(2), 125-150, https://doi.org/10.1016/S1463-5003(02)00063-X

Debreu, L., Marchesiello, P., Penven, P., and Cambon, G. (2012). Two-way nesting in split-explicit ocean models: Algorithms, implementation and validation. Ocean Modelling, 49, 1-21, https://doi.org/10.1016/j.ocemod.2012.03.003

Debreu, L., Vouland, C., and Blayo, E. (2008). AGRIF: Adaptive grid refinement in Fortran. Computers & Geosciences, 34(1), 8-13, https://doi.org/10.1016/j.cageo.2007.01.009

De Mey-Frémaux and the Groupe MERCATOR Assimilation (1998). Scientific Feasibility of Data Assimilation in the MERCATOR Project. Technical Report, doi: https://doi.org/10.5281/zenodo.3677206

De Mey P., Craig P., Kindle J., Ishikawa Y., Proctor R., Thompson K., Zhu J., and contributors (2007). Towards the assessment and demonstration of the value of GODAE results for coastal and shelf seas and forecasting systems, 2nd ed. GODAE White Paper, GODAE Coastal and Shelf Seas Working Group (CSSWG), 79 pp. Available online at: http://www.godae.org/CSSWG.html

De Mey-Frémaux, P., Ayoub, N., Barth, A., Brewin, R., Charria, G., Campuzano, F., Ciavatta, S., Cirano, M., Edwards, C.A., Federico, I., Gao, S., Garcia-Hermosa, I., Garcia-Sotillo, M., Hewitt, H., Hole, L.R., Holt, J., King, R., Kourafalou, V., Lu, Y., Mourre, B., Pascual, A., Staneva, J., Stanev, E.V., Wang, H. and Zhu X. (2019). Model-Observations Synergy in the Coastal Ocean. Frontiers in Marine Science, 6:436, https://doi.org/10.3389/fmars.2019.00436

Desroziers, G., Berre, L., Chapnik, B., Poli, P. (2005). Diagnosis of observation, background and analysis-error statistics in observation space. Quarterly Journal of the Royal Meteorological Society, 131, 3385-3396, http://dx.doi.org/10.1256/qj.05.108

Dyke, P. (2016). Modelling Coastal and Marine Processes. 2nd Edition, Imperial College Press, https://doi.org/10.1142/p1028

Ebert, E. E. (2009). Neighborhood verification - a strategy for rewarding close forecasts. Weather and Forecasting, 24(6), 1498-1510, https://doi.org/10.1175/2009WAF2222251.1

Evensen, G. (2003). The ensemble Kalman filter: Theoretical formulation and practical implementation. Ocean dynamics, 53, 343-367, https://doi.org/10.1007/s10236-003-0036-9

Fox-Kemper, B., Adcroft, A., Böning, C.W., Chassignet, E.P., Curchitser, E., Danabasoglu, G., Eden, C., England, M.H., Gerdes, R., Greatbatch, R.J., Griffies, S.M., Hallberg, R.W., Hanert, E., Heimbach, P., Hewitt, H.T., Hill, C.N., Komuro, Y., Legg, S., Le Sommer, J., Masina, S., Marsland, S.J., Penny, S.G., Qiao, F., Ringler, T.D., Treguier, A.M., Tsujino, H., Uotila, P., and Yeager, S.G. (2019). Challenges and Prospects in Ocean Circulation Models. Frontiers in Marine Science, 6:65, https://doi.org/10.3389/fmars.2019.00065

Gerya, T. (2019). Introduction to Numerical Geodynamic Modelling. 2nd edition, Cambridge University Press, https://doi.org/10.1017/9781316534243

Ghantous, M., Ayoub, N., De Mey-Frémaux, P., Vervatis, V., Marsaleix, P. (2020). Ensemble downscaling of a regional ocean model. Ocean Modelling, 145, http://dx.doi.org/10.1016/j.ocemod.2019.101511

Ghil, M., and Melanotte-Rizzoli, P. (1991). Data Assimilation in Meteorology and Oceanography. Advances in Geophysics, 33, 141-266, https://doi.org/10.1016/S0065-2687(08)60442-2

Greenberg, D.A., Dupont, F., Lyard, F., Lynch, D., Werner, F. (2007). Resolution issues in numerical models of oceanic and coastal circulation. Continental Shelf. Research, 27(9), https://doi.org/10.1016/j.csr.2007.01.023

Griffies, S. M., Pacanowski, R. C., and Hallberg, R. W. (2000). Spurious diapycnal mixing associated with advection in a z-coordinate ocean model. Monthly Weather Review, 128, 538-564, https://doi.org/10.1175/1520-0493(2000)128<0538:SDMAWA>2.0.CO;2

Griffies, S. M. (2006). Some ocean model fundamentals. In "Ocean Weather Forecasting", Editoris: E. P. Chassignet and J. Verron, 19-73, Springer-Verlag, Dordrecht, The Netherlands, doi:10.1007/1-4020-4028-8_2

Hallberg, R. (2013). Using a resolution function to regulate parameterizations of oceanic mesoscale eddy effects. Ocean Modelling, 72, 92-103, https://doi.org/10.1016/j.ocemod.2013.08.007

Hersbach H. (2000). Decomposition of the continuous ranked probability score for ensemble prediction systems. Weather and Forecasting, 15(5), 559-570, https://doi.org/10.1175/1520-0434(2000)015<0559:DOTCRP>2.0.CO;2

Herzfeld, M., and Gillibrand, P.A. (2015). Active open boundary forcing using dual relaxation time-scales in downscaled ocean models. Ocean Modelling, 89, 71-83, https://doi.org/10.1016/j.ocemod.2015.02.004

Hewitt, H.T., Roberts, M., Mathiot, P. et al. (2020). Resolving and Parameterising the Ocean Mesoscale in Earth System Models. Current Climate Change Reports, 6, 137-152, https://doi.org/10.1007/s40641-020-00164-w

Hirsch, C. (2007). Numerical Computation of Internal and External Flows - The Fundamentals of Computational Fluid Dynamics. 2nd Edition, Butterworth-Heinemann.

Hunke, E., Allard, R., Blain, P., Blockey, E., Feltham, D., Fichefet, T., Garric, G., Grumbine, R., Lemieux, J.-F., Rasmussen, T., Ribergaard, M., Roberts, A., Schweiger, A., Tietsche, S., Tremblay, B., Vancoppenolle, M., Zhang, J. (2020). Should Sea-Ice Modeling Tools Designed for Climate Research Be Used for Short-Term Forecasting? Current Climate Change Reports, 6, 121-136, https://doi.org/10.1007/s40641-020-00162-y

Ide, K., Courtier, P., Ghil, M., and Lorenc, A. C. (1997). Unified notation for data assimilation: Operational, sequential and variational (Special Issue Data Assimilation in Meteorology and Oceanography: Theory and Practice). Journal of the Meteorological Society of Japan, Ser. II, 75(1B), 181-189, https://doi.org/10.2151/jmsj1965.75.1B_181

Janssen, P.A.E.M., Abdalla, S., Hersbach, H., Bidlot, J.R. (2007). Error estimation of buoy, satellite, and model wave height data. Journal of Atmospheric and Oceanic Technology, 24(9), 1665-1677, https://doi.org/10.1175/JTECH2069.1

Juricke, S., Lemke, P., Timmermann, R., Rackow, T. (2013). Effects of Stochastic Ice Strength Perturbation on Arctic Finite Element Sea Ice Modeling. Journal of Climate, American Meteorological Society, 26(11), 3785-3802, https://doi.org/10.1175/JCLI-D-12-00388.1

Kantha, L. H., & Clayson, C. A. (2000). Numerical models of oceans and oceanic processes. Elsevier, 1-940, ISBN: 978-0-12-434068-8.

Katavouta, A., Thompson, K.R. (2016). Downscaling ocean conditions with application to the Gulf of Maine, Scotian Shelf and adjacent deep ocean. Ocean Modelling, 104, 54-72, https://doi.org/10.1016/j.ocemod.2016.05.007

Lamouroux, J., Charria, G., Mey, P. De, Raynaud, S., Heyraud, C., Craneguy, P., Dumas, F., Le Hénaff, M. (2016). Objective assessment of the contribution of the RECOPESCA network to the monitoring of 3D coastal ocean variables in the Bay of Biscay and the English Channel. Ocean Dynamics, 66(4), 567-588, http://dx.doi.org/10.1007/s10236-016-0938-y

Latif, M., Barnett, T.P., Cane, M.A. et al. (1994). A review of ENSO prediction studies. Climate Dynamics, 9, 167-179.

Le Traon, P. Y., Reppucci, A., Alvarez Fanjul, E., Aouf, L., Behrens, A., Belmonte, M., ... and Zacharioudaki, A. (2019). From observation to information and users: the Copernicus Marine Service perspective. Frontiers in Marine Science, 6, 234, https://doi.org/10.3389/fmars.2019.00234

Lellouche, J.-M., Le Galloudec, O., Drévillon, M., Régnier, C., Greiner, E., Garric, G., Ferry, N., Desportes, C., Testut, C.-E., Bricaud, C., Bourdallé-Badie, R., Tranchant, B., Benkiran, M., Drillet, Y., Daudin, A., De Nicola, C. (2013). Evaluation of global monitoring and forecasting systems at Mercator Océan. Ocean Science, 9, 57-81, 2013, https://doi.org/10.5194/os-9-57-2013

Lima, L.N., Pezzi, L.P., Penny, S.G., and Tanajura, C.A.S., (2019). An investigation of ocean model uncertainties through ensemble forecast experiments in the Southwest Atlantic Ocean. Journal of Geophysical Research: Oceans, 124, 432-452. https://doi.org/10.1029/2018JC013919

Lumpkin, R., and Speer, K. (2007). Global Ocean Meridional Overturning. Journal of Physical Oceanography, 37(10), 2550-2562, https://doi.org/10.1175/JPO3130.1

Lyard, F. H., Allain, D. J., Cancet, M., Carrere, L., and Picot, N. (2021). Fes2014 global ocean tides atlas: design and performances. Ocean Science, 17, 615-649, https://doi.org/10.5194/os-17-615-2021

Madec, G., and NEMO System Team, (2022). "NEMO ocean engine", Scientific Notes of Climate Modelling Center (27) – ISSN 1288-1619, Institut Pierre-Simon Laplace (IPSL), doi:10.5281/zenodo.6334656

Martin, M. J., Hines, A., and Bell, M. J. (2007). Data assimilation in the FOAM operational short-range ocean forecasting system: a description of the scheme and its impact. Quarterly Journal of the Royal Meteorological Society, 133(625), 981-995, https://doi.org/10.1002/qj.74

Martin, M. J., Balmaseda, M., Bertino, L., Brasseur, P., Brassington, G., Cummings, J., ... and Weaver, A. T. (2015). Status and future of data assimilation in operational oceanography. Journal of Operational Oceanography, 8(sup1), s28-s48, https://doi.org/10.1080/1755876X.2015.1022055

Mason, E., Pascual, A., and McWilliams, J.C. (2014). A new sea surface height–based code for oceanic mesoscale eddy tracking. Journal of Atmospheric and Oceanic Technology, 31(5), 1181-1188, https://doi.org/10.1175/JTECH-D-14-00019.1

Mazloff, M. R., Cornuelle, B., Gille, S. T., Wang, J. (2020). The importance of remote forcing for regional modeling of internal waves. Journal of Geophysical Research: Oceans, 125, e2019JC015623, https://doi.org/10.1029/2019JC015623

Menard, R., and Daley, R. (1996). The application of Kalman smoother theory to the estimation of 4DVAR error statistics. Tellus A: Dynamic Meteorology and Oceanography, 48, 221-237, https://doi.org/10.3402/tellusa.v48i2.12056

Mittermaier, M., Roberts, N., and Thompson, S.A. (2013). A long-term assessment of precipitation forecast skill using the Fractions Skill Score. Meteorological Applications, 20(2), 176-186, https://doi.org/10.1002/met.296

Mittermaier, M., North, R., Maksymczuk, J., Pequignet, C., & Ford, D. (2021). Using feature-based verification methods to explore the spatial and temporal characteristics of forecasts of the 2019 Chlorophyll-a bloom season over the European North-West Shelf. Ocean Science, 17, 1527-1543, https://doi.org/10.5194/os-17-1527-2021

Mogensen, K, Balmaseda, A., Alonso, W.M. (2012). The NEMOVAR ocean data assimilation system as implemented in the ECMWF ocean analysis for System 4. Technical memorandum, doi:10.21957/x5y9yrtm

O'Brien, M.P., and Johnson, J.W. (1947). Wartime research on waves and surf. The Military Engineer, 39, pp. 239-242.

Oke, P. R., Brassington, G. B., Griffin, D. A., and Schiller, A. (2008). The Bluelink ocean data assimilation system (BODAS). Ocean Modelling, 21(1-2), 46-70, https://doi.org/10.1016/j.ocemod.2007.11.002

Ollinaho, P., Lock, S., Leutbecher, M., Bechtold, P., Beljaars, A., Bozzo, A., Forbes, R.M., Haiden, T., Hogan, R.J., Sandu, I. (2017). Towards process-level representation of model uncertainties: stochastically perturbed parametrizations in the ECMWF ensemble. Quarterly Journal of the Royal Meteorological Society, 143, 408-422, http://dx.doi.org/10.1002/qj.2931

Palmer, T. (2018). The ECMWF ensemble prediction system: Looking back (more than) 25 years and projecting forward 25 years. Quarterly Journal of the Royal Meteorological Society, 145, 12-24, https://doi.org/10.1002/qj.3383

Penduff, T., Barnier, B., Terray, L., Sérazin, G., Gregorio, S., Brankart, J.-M., Moine, M.-P., Molines, J.-M., Brasseur, P. (2014). Ensembles of eddying ocean simulations for climate. In: CLIVAR Exchanges, 65(19), 26-29. Available at: https://www.clivar.org/sites/default/files/documents/exchanges65_0.pdf

Pham, D. T., Verron, J., and Roubaud, M.C. (1998). A singular evolutive Kalman filters for data assimilation in oceanography. Journal of Marine Systems, 16(3-4), 323-340, https://doi.org/10.1016/S0924-7963(97)00109-7

Pinardi, N., Lermusiaux, P.F.J., Brink, K.H., Preller, R. H. (2017). The Sea: The science of ocean predictions. Journal of Marine Research, 75(3), 101-102, https://doi.org/10.1357/002224017821836833

Quattrocchi, G., De Mey, P., Ayoub, N., Vervatis, V., Testut, C.-E., Reffray, G., Chanut, J., Drillet, Y., (2014). Characterisation of errors of a regional model of the bay of biscay in response to wind uncertainties: a first step toward a data assimilation system suitable for coastal sea domains. Journal of Operational Oceanography, 7(2), 25-34, https://doi.org/10.1080/1755876X.2014.11020156

Ren, S., Zhu, X., Drevillon, M., Wang, H., Zhang, Y., Zu, Z., Li, A. (2021). Detection of SST Fronts from a High-Resolution Model and Its Preliminary Results in the South China Sea. Journal of Atmospheric and Oceanic Technology, 38(2), 387-403, https://doi.org/10.1175/JTECH-D-20-0118.1

Ryan, A. G., Regnier, C., Divakaran, P., Spindler, T., Mehra, A., Smith, G. C., et al. (2015). GODAE OceanView Class 4 forecast verification framework: global ocean inter-comparison. Journal of Operational Oceanography, 8(sup1), S112-S126, https://doi.org/10.1080/1755876X.2015.1022330

Sakov, P., Counillon, F., Bertino, L., Lisæter, K.A., Oke, P.R., Korablev, A., (2012). TOPAZ4: an ocean-sea ice data assimilation system for the north atlantic and arctic. Ocean Science, 8 (4), 633–656, http://dx.doi.org/10.5194/os-8-633-2012

Sandery, P.A., and Sakov, P. (2017). Ocean forecasting of mesoscale features can deteriorate by increasing model resolution towards the submesoscale. Nature Communications, 8, 1566, http://dx.doi.org/10.1038/s41467-017-01595-0

Santana-Falcón, Y., Brasseur, P., Brankart, J.M., and Garnier, F. (2020). Assimilation of chlorophyll data into a stochastic ensemble simulation for the North Atlantic Ocean. Ocean Science, 16, 1297-1315, https://doi.org/10.5194/os-16-1297-2020

Sasaki, Y. (1970). Some basic formalisms in numerical variational analysis. Monthly Weather Review, 98(12), 875-883.

Sein, D.V., Koldunov, N.K., Danilov, S., Wang,Q., Sidorenko, D., Fast, I., Rackow, T., Cabos, W., Jung, T. (2017). Ocean Modelling on a Mesh With Resolution Following the Local Rossby Radius. Journal of Advances in Modelling Earth Systems, 9:7, 2601-2614, https://doi.org/10.1002/2017MS001099

Simon, E., and Bertino, L. (2009). Application of the Gaussian anamorphosis to assimilation in a 3-D coupled physical-ecosystem model of the North Atlantic with the EnKF: a twin experiment. Ocean Science, 5, 495-510, 2009, https://doi.org/10.5194/os-5-495-2009

Smith, G.M., Roy, F., Reszka, M., Surcel Colan, D., He, Z., Deacu, D., Belanger, J.-M., Skachko,S., Liu, Y., Dupont, F., Lemieux, J.-F., Beaudoin, C., Tranchant, B., Drévillon, M., Garric, G., Testut, G.-E., Lellouche, J.-M., Pellerin, P., Ritchie, H., Lu, Y., Davidson, F., Buehner, M., Caya, A., Lajoie, M. (2016). Sea ice forecast verification in the Canadian Global Ice Ocean Prediction System. Quarterly Journal of the Royal Meteorological Society, 142(695), 659-671, https://doi.org/10.1002/qj.2555

Storto, A., and Andriopoulos, P., (2021). A new stochastic ocean physics package and its application to hybrid-covariance data assimilation. Quarterly Journal of the Royal Meteorological Society, 147, 1691-1725, https://doi.org/10.1002/qj.3990

Tchonang, B.C., Benkiran, M., Le Traon P.-Y., Van Gennip, S.J., Lellocuhe, J.M., Ruggiero, G. (2021). Assessing the impact of the assimilation of SWOT observations in a global high-resolution analysis and forecasting system. Part 2: Results. Frontiers in Marine Science, 8:687414, https://doi.org/10.3389/fmars.2021.687414

Thacker, W.C., Srinivasan, A., Iskandarani, M., Knio, O.M., Le Hénaff, M., (2012). Propagating boundary uncertainties using polynomial expansions. Ocean Modelling, 43-44, 52-63, http://dx.doi.org/10.1016/j.ocemod.2011.11.011

Thoppil, P.G., Frolov, S., Rowley, C.D. et al. (2021). Ensemble forecasting greatly expands the prediction horizon for ocean mesoscale variability. Communications Earth & Environment, 2, 89, https://doi.org/10.1038/s43247-021-00151-5

Toublanc, F., Ayoub, N.K., Lyard, F., Marsaleix, P., Allain, D.J., 2018. Tidal downscaling from the open ocean to the coast: a new approach applied to the Bay of Biscay. Ocean Modelling, 214, 16-32. http://dx.doi.org/10.1016/j.ocemod.2018.02.001

Usui, N., Ishizaki, S., Fujii, Y., Tsujino, H., Yasuda, T., Kamachi, M. (2006). Meteorological Research Institute multivariate ocean variational estimation (MOVE) system: Some early results. Advances in Space Research, 37(4), 806-822, https://doi.org/10.1016/j.asr.2005.09.022

Vervatis, V. D., Testut, C.E.. De Mey, P., Ayoub, N., Chanut, J., Quattrocchi, G. (2016). Data assimilative twin-experiment in a high-resolution Bay of Biscay configuration: 4D EnOI based on stochastic modelling of the wind forcing. Ocean Modelling, 100, 1-19, https://doi.org/10.1016/j.ocemod.2016.01.003

Vervatis, V.D., De Mey-Frémaux, P., Ayoub, N., Karagiorgos, J., Ciavatta, S., Brewin, R., Sofianos, S., (2021a). Assessment of a regional physical-biogeochemical stochastic ocean model. Part 2: empirical consistency. Ocean Modelling, 160, 101770, http://dx.doi.org/10.1016/j.ocemod.2021.101770

Vervatis, V. D., De Mey-Frémaux, P., Ayoub, N., Karagiorgos, J., Ghantous, M., Kailas, M., Testut, C.-E., and Sofianos, S., (2021b). Assessment of a regional physical-biogeochemical stochastic ocean model. Part 1: ensemble generation. Ocean Modelling, 160, 101781, https://doi.org/10.1016/j.ocemod.2021.101781

Waters, J., Lea, D.L., Martin, M.J., Mirouze, I., Weaver, A., While, J. (2014). Implementing a variational data assimilation system in an operational 1/4 degree global ocean model. Quarterly Journal of the Royal Meteorological Society, 141(687), 333-349, https://doi.org/10.1002/qj.2388

Zaron, E.D. (2011). Introduction to Ocean Data Assimilation. In: Schiller, A., Brassington, G. (eds) "Operational Oceanography in the 21st Century". Springer, Dordrecht. https://doi.org/10.1007/978-94-007-0332-2_13